Spectrum of Engineering Sciences
ISSN (e) 3007-3138 (p) 3007-312X Volume 3, Issue 12, 2025

# HYBRID PRINTED ENERGY SYSTEMS: INTEGRATING FLEXIBLE SOLAR CELLS WITH ON-BODY ENERGY STORAGE

[1]Md. Moniruzzaman Anik, [2]Faateh Ibrahim
[1-2]Wuhan Textile, University Sunshine Campus, China
[1]monir.anik47@gmail.com, [2]Faateh77@gmail.com

DOI: https://doi.org/10.5281/zenodo.18109105

**Keywords:**
Hybrid Printed Energy System, Flexible Perovskite Solar Cells, Zinc-Ion Storage, Wearable Electronics, Additive Manufacturing

**Article History**
*Received on 18 Nov, 2025*
*Accepted on 25 Dec 2025*
*Published on 29 Dec 2025*


**Corresponding Author:**

## Abstract

*This study presents the design, fabrication, and characterization of a hybrid printed energy system that integrates flexible perovskite solar cells (PSCs) with zinc-ion on-body energy storage units. Utilizing a scalable inkjet printing and low temperature annealing, the system had a power conversion efficiency (PCE) of 16.8%, an open circuit voltage of 1.07 V and a fill factor of 74.1% under standard AM1.5G illumination. The areal capacitance, energy density and power density of the integrated zinc ion capacitor were 1.65 F/cm², 66.10 mWh/cm², and 21.5 mW/cm², respectively, and >95% capacitance retention was achieved after 5000 cycles. Direct photovoltaic power absorption coupling Now with the direct photovoltaic welding coupling with storage, a 91.4% charge transfer efficiency is achieved, and overall efficiency of 14.8%, demonstrating excellent energy charging phenomenon and real-time full-time charge ability; mechanical toughening the bending of >10,000 cycles, and more than 90% performance reserve. Statistical analysis ($R^2$ = 0.91) assured good predictive reliability between morphological uniformity and electrical output and the validation by simulation (with a root mean square error (RMSE < 3%) assured the accuracy of the model. The results lay the foundation for a robust, flexible and eco-friendly power platform that can be used for wearable and biomedical electronics, and create the way for large gardens scale sustainable energy integration using printed technologies.*

## Chapter 1: Introduction

### 1.1 Background and Context

The world energy landscape is in the midst of a massive transformation spurred by the need to adapt fossil-fuel-based energy systems into sustainable, decentralized and renewable energy sources in a desperate bid to slow down the effects of climate change. As global population growth, industrialization and urbanization continue to escalate, energy demand is expected to grow a lot. Traditional centralized grids, which are mainly based on nonrenewable sources such as coal, natural gas, and oil, are part of the problem with greenhouse gasses and environmental degradation, and there is a hastened move towards renewable energy technologies. Decentralized energy systems that include solar photovoltaics (PV), wind turbines, micro-hydro systems, and hybrid energy systems are becoming more widely acknowledged as essential components in matters of energy accessibility, resilience, and sustainability in both urban and rural settings. These systems technically minimize transmission losses, enable energy autonomy on a local scale and are in line with the goals of climate change mitigation through lessening relations to centralized energy infrastructures and fossil fuels (Laugs et al. 2024).

Solar energy is unique among all different types of renewable energy sources in its scalability, its versatility, and in the sheer number of solar panels available across the planet. Photovoltaic technology, in most cases, has taken since to behave continuously, progressing from "old rigid" crystalline silicon-based photovoltaic panels to extremely flexible, thin-film, and printable variants that can be incorporated into various surfaces and environments. Flexible photovoltaics are the cutting edge for this transition, and are needed for lightweight, conformable and wearable power generation solutions. These systems are not only capable of powering stationary and mobile applications, but they also promise to revolutionize human-technology interaction by energy-autonomous wearable devices. Flexible solar cells with perovskite and organic compositions have power conversion efficiencies of over 24%, whilst still retaining resiliency and adaptability for incorporation into curved and irregular surfaces (Ahmed & Hashem, 2025). The roll-to-roll fabrication of these cells has boosted their chances for mass production and therefore provides a cost-effective route to widespread deployment (Maoz et al., 2025).

The spread of decentralized and mobile energy systems has also been boosted by the development of hybrid systems combining energy harvesting and storage. For example, the hybrid solar-hydro or solar-battery microgrids have been successfully put in place in rural electrification projects optimizing cost and reliability while minimizing the effective cost of generating electricity per unit (levelized cost of electricity) and intrusiveness to large-scale grid infrastructure (Iweh et al., 2024; Ugwoke et al., 2020). Such systems are excellent examples of the strategic value of decentralization, especially for off-grid and low-income communities, where renewable hybrid mini-grids are sustainable solutions for domestic and productive uses. Decentralized Systems updated for Better Resilience Balance the fluctuating output of variable renewable generation synonymous with fluctuating environmental conditions using local storage mechanism is the key to resilient energy supply system, Fraderic's vision of continuous energy supply even in fluctuating environmental conditions is summarized as follows in Laugs et al. (2024). In addition to fixed systems, a big step ahead of more renewable energy gathering linked with high-tech materials and pliable electronics have given rise to a novel scenario in the realm of the worn and the on-body systems. Wearable electronics, which includes smart textiles, medical sensors, and human-machine interface, require autonomous, low-weight and unobtrusive power sources, which can function without traditional batteries or wired power. The limitations of conventional lithium ion batteries such as rigidity, charge cycles and safety aspects have led to the development of flexible and integrated energy platforms that integrate energies harvesting from renewable and on-body energy storage (Saifi et al., 2024; Jahandar and Kim, 2024). These hybrid printed energy systems therefore promise not only enhanced user comfort and mobility, but develop the self-supporting wearable electronic devices with capability to operate continuously in various environmental conditions.

The development of flexible integration of photovoltaic modules into flexible substrates has been accompanied by the development of the technology of energy storage technologies. Printed zinc-ion, magnesium-ion and lithium-ion microcapacitors are among the latest achievements towards compact, flexible and safe on-body power systems (Zeng et al., 2020; Tian et al., 2019). These devices have a high capacitance, rapid charging ability and stable cyclic performance, which make them suitable for direct coupling with printed solar cells with a single integrated platform. The overall efficiency of such hybrid units that use the combination of photoelectric conversion and electrochemical storage has been up to 17.8%, proving the feasibility of fully printed, mechanically robust, and energy-autonomous wearable systems (Zeng et al., 2020). Moreover, the introduction of magnesium-ion quasi-solid-state supercapacitors to further

improve energy density, safety, and current tolerance to solve the problems of bulky interconnections and thermal management for wearable applications (Tian et al., 2019). The packing more and more electronics into smaller and smaller volume and the omnipresence of body sensory webs (bodyNETs) have highlighted the significance of sustainable power supplies capable of driving physiology monitoring continuously, health screening and interactive functionalities. Traditional battery powered wearables are limited by their charging frequency and their effect on the environment, which has driven the research into hybrid energy harvesters that are able to simultaneously harvest multiple types of energy such as solar, thermal, mechanical and radiofrequency within a single device architecture (He et al., 2020). By combining different energy conversion mechanisms, such hybrid systems help to maximize energy availability, guarantee longer operational life times and minimize electronic waste. The fusion of nanogenerators, supercapacitors and solar cells are the examples of this direction, which provides multifunctional energy solutions thanks to piezoelectric, triboelectric and photovoltaic effects to achieve seamless power generation and storage (Hajra et al., 2024).

Wearable electronics have no less role to play in the overall energy transition. As society comes to embrace pervasive computing, health monitoring and digital interconnectivity, the need for autonomous, body-conformal power systems becomes less important. Ultra-flexible energy harvesting and storage technologies that noticeably suffered from poor mechanical compliance in recent years are increasingly introduced with outstanding mechanical compliance. Because devices with a low thickness of 90 μm were able to sustain high energy density (5.82 mWh $cm^{-2}$) and energy conversion efficiency (16%) under dynamic motion,18 Saifi et al. recently showed the potential as a new energy harvesting and storage device. Such systems are a concrete step towards the realization of sustainable, self-powered wearable devices that are in line with efforts across the world to lessen energy use and environmental impact. The incorporation of such technologies in the form of photovoltaic fabrics and smart energy harvesting in garments only adds more magnitude to the potential of their continuous power generation in real-world scenarios (Ali et al., 2024).

Printed electronics is playing a pivotal role in the large scale realisation of these hybrid energy systems. Conductive patterns, electrodes and active layers can be fabricated on flexible substrates in high precision and at low cost through such techniques as inkjet, screen, gravure printing and so on. The flexibility of these approaches for low-temperature and scalable fabrication processes is in favor of their use in the fabrication of integrated systems for application in wearable and biomedical systems. Moreover, printed energy devices provide unique mechanical advantages, such as stretchability and conformability that are essential in order to keep performance under continuous motion or deformation (Zeng et al., 2020; Tian et al., 2019). The convergence of printing technology and engineering of nanomaterials has resulted in emergence of advanced functional inks with the content of carbon nanostructures, metal oxides and conductive polymers with superior electrical conductivity and mechanical resilience.

The current advancement in flexible perovskite and organic solar cells has strengthened the technological supporting base of hybrid printed mechanisms. Flexible quasi-two-dimensional perovskite solar cells, for example, have achieved certain power outputs as high as 44 W $g^{-1}$ and operational efficiencies over 20% all while maintaining climatic mechanical half-life and environmental steadiness (Hailegnaw et al. 2024). These advancements are not only catered to wearable technology but also spread out to portable autonomous systems like drones and IoT devices. Similarly, flexible organic photovoltaics that are combined with thin-film batteries or supercapacitor have been mapped as transformative elements as wearable energy autonomy components that can be used to enable seamless supply from power sources, without bulky or rigid components (Jahandar & Kim, 2024).

At the macro scale, it can be seen that decentralized energy systems are really about the same principles of autonomy and adaptability as the wearable power technologies. Both domains are focused on efficiency, resilience and sustainability by way of modular integration and local energy management. The use of hybrid microgrids that incorporate a mix of solar, wind and storage is similar to the functional design of hybrid wearable systems where multiple energy inputs are harmonized to ensure continuous power supply and stability (Laugs et al, 2024). Furthermore, the use of hybrid storage technologies like combination of electrochemical and molecular storage in localized grid enhances the self-sufficiency of energy usage which in turn reduces the dependency on external networks, analogous to the function of the on-body hybrid energy units which combine energy harvesting and storage to ensure uninterrupted energy operation.

One of the trends that is increasingly highlighted between sustainable energy systems and wearable electronics is a larger paradigm shift as we move toward the concept of

distributed, user-based power generation. Innovations in printed and flexible electronics have enabled the democratization of energy production to allow a person to create and store energy, themselves, in their bodies, their clothing or their personal devices. This shift not only decentralizes energy infrastructure but also goes with the circular economy principles of focusing on energy efficiency, making materials more recyclable and having less of an impact on the environment. Flexible solar cells and printed energy storage devices are collectively the basis of this movement towards the personal and sustainable energy ecosystem (Maoz et al., 2025; Ahmed & Hashem, 2025).

In the future, the marriage of flexible photovoltaics and an on-body energy storage will further emphasize the limitation of wearable technology and sustainable integration of energy, the interaction of technology, as well as the power pipeline. The ability to manufacture fully printed, light-weight and high-performing hybrid systems makes way for ubiquitous energy solutions that are adaptable and scalable as well as environmentally benign. With the advancement of research on materials, architectures and manufacturing techniques, hybrid printed energy systems are expected to play a pivotal role not only in the powering wearable electronics but also in the move to decentralized and self-sufficient energy models around the world (Saifi et al., 2024; Ali et al., 2024; Jahandar & Kim, 2024).

1.2 Research Problem

Despite rapid developments in the flexible photovoltaics and printed energy storage technologies, the development of fully integrated, hybrid, printed energy systems that are capable of reliable on-body operation is very limited. Current wearable power solutions have low energy conversion and storage efficiency, mechanical instability during repeated deformation and incompatibility between solar harvesting and storage modules. Moreover, scalable and secure methods for the fabrication of such hybrid systems have still not been developed. Therefore, there is an urgent need to design and optimize mechanically robust and high-efficiency hybrid printed energy system that seamlessly combines flexible solar cells and on-body energy storage with a continuous and autonomous power generation for wearable and biomedical applications.

**1.3 Research Questions**

- How can printed flexible solar cells be effectively integrated with on-body energy storage systems?
- What materials, interfaces, and printing methods enable mechanical flexibility and stability?
- What is the optimal configuration for maximizing energy transfer efficiency and durability?

1.4 Research Objectives

- Develop and characterize a hybrid printed energy system.
- Evaluate the performance (electrical, mechanical, and thermal) of the integrated device.
- Analyze real-world performance under simulated on-body conditions.

**Chapter 2: Literature Review**

**2.1 Overview of Printed Electronics**

Printed electronics can be seen as a revolutionary development from the use of subtractive fabrication techniques to additive and sustainable and cost efficient manufacturing of functional electronics. Unlike traditional microelectronics that are based on vacuum deposition and photolithography, printed electronics makes use of solution-based deposition techniques to create conductive, semiconductive or dielectric layers on flexible substrates. Among the most popular of these printing technologies, inkjet, screen, gravure and aerosol jet printing have become the most widely used among flexible energy systems. Each of these methods has its own advantages based on the resolution, scalability and compatibility with various materials. The digital printing technology, commonly referred to as inkjet printing, is a digital patterning technology that allows for the formation of patterns using droplet ejection without the use of masks, and provides excellent material utilization and design flexibility (Peng et al., 2017). This type of technique is especially efficient when applied to multilayer device structures such as organic and perovskite solar cells and printed batteries or devices with emitted light, as control of film thickness and morphology is critical in devices with varying efficiencies (Mitra et al., 2018).

Screen printing on the other hand offers a sturdy and scalable method for printing thick functional layers such as the electrodes or dielectric barrier. Its adaptability to large scale, roll-the-roll processes makes this very suitable for industrial scale energy devices. Recent innovations have led to the optimization of screen-printed vias with silver microparticle inks for flexible modules with outstanding result of 30 000 bending cycles, which is excellent for high-durability energy harvesting systems (Kujala et al. 2020). Gravure printing for its high print speed and fine line patterning has been setting new standards in the large-area electronics manufacturing industry. It allows constant coating of functional materials, especially for conductive inks for solar and storage devices, which allows for the fast production of flexible circuits (Aleeva & Pignataro, 2014). Aerosol jet printing, meanwhile, helps in the direct deposition of nanoscopic features in the deposition of features to non-

planar surfaces. The method has been shown to have exceptional versatility when used to fabricate ternary nanocomposites such as PEDOT:PSS with graphene oxide, and has resulted in films with enhanced specific capacitance and electrochemical stability and could prove useful in the fabrication of high performance printed supercapacitors (Greco et al., 2023).

The move towards sustainable manufacturing practices in the evolution of the printing technologies is another defining trend. Additive printing has considerably lower material waste, energy and environmental toxicity compared to conventional lithographic methods. The approach also allows to minimize production steps by allowing direct material deposition only where necessary (Altay et al., 2020). As such, printed electronics are in line with international efforts towards green and circular manufacturing, and provide environmentally friendly alternatives for the production of devices across the range of photovoltaics, sensors and batteries. This transformation towards green fabrication process is being aided by the combination of artificial intelligence and additive manufacturing tools, which optimize and make the fabrication of printed circuits and devices reproducible (Chen et al., 2025).

The choice of the conductive inks and substrates assigned an important role to how well the printed electronics will perform and how reliable they will be. Conductive inks normally consist of metallic nanoparticles (Ag, Cu), carbon nanomaterials (graphene, CNTs) as well as conductive polymers such as PEDOT:PSS or polyaniline (PANI). Among them, PEDOT:PSS has become ubiquitous because of its high electrical conductivity, optical transparency and low temperature processing compatibility. Recent research has shown the improved electrochemical properties of PEDOT:PSS/graphene oxide nanocomposites, which show capacitance values in excess of 31 F/g and a better cyclic stability, proving that these materials can be used in printed energy storage applications (Greco et al., 2023). Similarly, PANI based conductive inks possess tunable electrical properties by doping and additive modification procedures to be applicable for flexible supercapacitor, electrochromic and biosensors (Arora et al., 2023).

Flexible substrates are the backbone of the structure of printed devices. Some common materials are polyethylene terephthalate (PET), polyethylene naphthalate (PEN), polinyldeme (PI) and cellulose based papers. Paper substrates in particular have attracted the attention of researchers who are interested in low-cost and biodegradable substrates for flexible electronics, including flexible electronics. They are intrinsically porous and enable infiltration of electronics material to form hybrid substrates which comprise both mechanical and electrical properties. Devices by train on cellulosic based substrates have shown solar cell efficiencies as high as 13% and supercapacitor capacities of 1350 mF $cm^{-2}$, demonstrating the potential of paper as an environmentally benign basis for printed electronics (Brunetti et al., 2019). Combined these advancements have made the printed electronics a foundation of sustainable and flexible energy systems.

**2.2 Flexible and Printed Solar Cells**

Flexible and printed solar cell are a coming together of endeavors in material science, nanotechnology and manufacturing innovation. Unlike traditional rigid modules of photovoltaic cells, these devices use light weight, bendable substrates that allow the inclusion in wearables, fabric and curved surfaces. Among the most important classes are Organic Photovoltaics (OPV), Perovskite Solar Cells (PSC) and Dye-Sensitized Solar Cells (DSSC) which have unique benefits in terms of mechanical adaptability, cost efficiency and environmental sustainability. Organic solar cells (OSCs) have made progress on account of their solution processable polymers and fullerene or non-fullerene acceptors. Their compatibility with inkjet and gravure printing allows them to be printed or ink-jet printed with high throughput with little material losses. Printed OPV arrays using the inkjet technology has shown more than 85% yield in thousands of devices that proves the reproducibility in industrial manufacturing and potential for flexible architecture (Mitra et al., 2018).

Perovskite solar cells (PSCs) have taken the world of solar cells by storm with power conversion efficiencies (PCEs) of greater than 25%. Their high absorption coefficients, tunable band gaps, as well as ease of manufacturing favorably make them the common contender for printed photovoltaics. Slot-die, blade, spray, and gravure printing have developed ink formulations and techniques of large-area printing, which have made the scalable production of perovskite modules with over 21% PCEs to be achieved (Parida et al., 2022; Wang et al., 2021). Recent attempts have also focused on roll-to-roll processing and electrospray deposition (which improves film uniformity and minimizes waste of material). Electrospray printing in particular has the potential to provide tight control over the droplet size and evaporation dynamics, resulting in nanostructured active layers of comparable performance to spin coated films (Zhao & Deng, 2020).

Indoor and wearable photovoltaics have been other driving forces for the innovation of perovskite-based systems. Perovskite indoor photovoltaics have excellent light absorption capability and tunable bandgap under low light conditions than silicon and dye-sensitized ones.

With efficiencies reaching close to 25%, these devices are a reliable source of power for internet of things (IoT) applications and self-powered sensors (Wang et al., 2021). Complementary to perovskites, flexible DSSCs have been developed on the basis of monolithic solid-state architectures based on printed WGF textile. These devices exhibit stability under mechanical stress as well as high/low temperatures compatible with textile material substrates, with efficiencies of 0.4% under simulated sun conditions showing promise to be used in energy fabrics with wearable real-world applications (Liu et al, 2019).

Encapsulation and interfacial engineering are key factors to guaranteeing the long-term and operational stability of flexible solar cells. One of the issues that has been long present in flexible PSCs is the degradation from the intrusion of moisture and oxygen. Novel encapsulation schemes using barrier coatings, crosslinked polymers and nanolaminate structures have greatly increased the device lifetime. Solution-processed transparent electrodes including silver nanowire networks, graphene films and conductive oxides are currently replacing brittle indium tin oxide (ITO) layers and have made high transparency and flexibility possible (Zhang et al., 2020; Ravikumar & Dangate, 2024). The combination of the flexible transparent electrodes and the stretchable organic optoelectronic devices is driving the limits of wearable and portable photovoltaic devices and therefore can be integrated into medical devices, e-skins and soft robotics (Ravikumar & Dangate, 2024).

Continuous innovation in areas of materials continue to lead to performance improvements. Perovskite and organic cells printed by inkjet have given efficiencies from 18% to 29% with stability under illumination conditions (Panidi et al. 2022). The optimization of the composition of hybrid perovskites, interface layers and defect passivation techniques has led to an additional improvement of the mechanical and environmental endurance of flexible modules. For example, flexible PSCs on polymer substrates with low-temperature processing (<150°C) have shown PCEs of 15.6%, and ultralight cells with fiber-based substrates have shown record power-to-weight ratios, which is a major step towards industrial scalability (Giacomo et al., 2016).

2.3 Printed Energy Storage Devices

Parallel to the development of printed photovoltaics, the production of printed energy storage devices such as batteries, supercapacitors and hybrid systems has developed very quickly. These devices give the critical ability to store the harvested energy from solar or mechanical energy, and give continuous operation to wearable and off-grid applications. Printed energy storage technologies are based to a large extent on the development of scalable deposition methods and novel materials with a balanced conductivity, capacitance and flexibility. Inkjet and screen printing are not only very well used to make electrodes but electrolytes and current collectors on flexible substrates to create small energy modules with high reliability.

Conductive polymers such as PEDOT:PSS and PANI, owing to their good flexibility, environmental stability and electrochemical activity, have become basic materials in printed energy storage. Polyaniline-base inks, Martin inks, through advanced improvements by doping with metal salts and halide ions have already achieved large specific capacitance values as well as stable charging/discharge behavior; these for high performance supercapacitors are viable. Similarly, PEDOT:PSS nanocomposites doped with graphene oxide showed great enhancement in charge storage and cyclic stability, on which next-generation printed electrochemical capacitors could be based (Greco et al., 2023).

Emerging research is also being conducted into hybrid structures for printable batteries/capacitor combination energy systems. The high-viscosity silver inks that can be used in screen printed vias guarantee excellent interconnectivity in multilayer energy modules with high bending resilience and suitability for roll-to-roll production (Kujala et al., 2020). Advances in additive manufacturing and 3D printing technology continue to broaden the prospect of making energy storage printed with extensive geometries and power embedded architecture settings that are essential for portable gadgets that function in need of conformal integration (Chen et al., 2025).

Material selection is therefore still a key factor in striking a balance between flexibility, capacity and durability. Carbon-based electrodes such as activated carbon, graphene and carbon nanotubes offer a high surface area to double-layer capacitance and transition metal oxides such as ($MnO_2$, ZnO)and conducting polymers offer pseudocapacitance. Hybrid systems make use of both mechanisms and provide better energy densities and still retain the mechanical flexibility. Paper-based energy storage devices are an example of such synergy that achieve specific capacities up to 2000 mAh $g^{-1}$and capacitances of 1350 mF $cm^{-2}$ while still being recyclable and inexpensive (Brunetti et al., 2019).

Looking into the future, printed storage systems are expected to do better because of advancements in solid electrolytes, nanostructured electrodes and encapsulation technologies. As flexible electronics keep developing, combining printed solar cells with such energy storage elements will develop fully self-sustaining systems to achieve wearables, IoT machines and autonomous

sensors. Combining high-efficiency printed photovoltaics and efficient printed supercapacitors is a new move in the right direction to achieve the ultimate objective of full-fledged engineered, sustainable and flexible energy systems.

2.4 Integration Strategies for Hybrid Systems

The incorporation of energy harvesting and storage devices in unifying adaptable hybrid systems is at the core of unifying self-sufficient wearable and textile-based energy solutions. Two dominating strategies of such integration approaches are direct coupling and indirect coupling of photovoltaic (PV) modules and storage units. The selection of integration topology has an important impact on the energy conversion efficiency, system complexity and mechanical durability. In direct coupling, both the solar cell and energy storage (battery or supercapacitor) are connected together without any intermediate circuitry and hence architecture is simple and cost of production is low. This type of approach depends upon impedance balancing for elimination of signal distortion between the photovoltaic output and the storage unit's charging characteristics in order to provide the finest power transfer. Direct coupling results in reduced requirement of maximum power point tracking (MPPT) electronics, therefore lowering system weight and volume - the need of flexibility and wearability in a flexible system makes it perfect for wearable applications. Studies show that efficient power matching can be achieved by properly tuned PV-battery system by using the battery as an intrinsic impedance matching component in the system across varying irradiance conditions. For example, Astakhov, Mahawith S, and O'Neal K. (2020) examined direct-coupled solar-battery units by modeling them and concluded that when integrated with power-matched configurations, were demonstrated to have a robust operation with varying irradiance levels and load resisters, and showed to be viable for scalable design with low complexity.

By contrast, indirect coupling uses a power management circuit which conventionally involves DC-DC converters, or MPPT systems, to optimize the energy taken from the solar cell and control the charging dynamics. While indirect coupling provides better energy efficiency and more operational flexibility, it adds further circuit complexity, higher fabrication cost and possible mechanical incompatibility with ultrathin substrates (Chaikaew & Punyawudho, 2021). Indirect coupling is favored in applications where there is a need for a precise energy regulation or operation in rapidly fluctuating illumination as in case of wearable medical sensors or outdoor textiles. In hybrid configurations of fuel cells and batteries, the optimal DC coupling voltage is important to achieve harmonized operation between the components; for example, an on-off coupling window of between 49-51 V was found to be the optimal value to maximize operational stability and transition time with no system failure (Chaikaew & Punyawudho, 2021).

Power management circuits have become more sophisticated to comply with the requirements of hybrid energy systems with variable working environments. In flexible solar rechargeable systems, integrated circuits with ease allow to switch between different energy harvesting, storage and consumption modes. These circuits are capable of dynamically balancing the input from solar cells and output towards load devices to ensure stable performance and also increase the lifetime of batteries. Hybrid management architectures with data-driven control algorithms like simultaneous perturbation stochastic approximation (SPSA) have been shown to be able to reduce power oscillations by more than 70% in hybrid systems, while reducing the battery degradation by up to 25% (Pelosi et al., 2024). The intelligent interconnection of supercapacitors and lithium-ion batteries in these power systems is a typical example of the transition towards adaptive power management with supercapacitors for rapid charge-discharge effects and then battery for long-term energy stability.

Recent progress in material science and structural design has opened the horizons of mechanically integrated hybrid systems. Saifi et al. (2024) reported on an ultra-flexible energy harvesting-storage system (FEHSS) incorporating the high performance organic photovoltaics and zinc-ion batteries in 90 um thick configuration. The system achieved a power conversion efficiency of more than 16%, a power output of 10 mW cm-2, and an energy density of more than 5.82 mWh cm-2, and at the same time, it still maintained mechanical integrity, even after being repeatedly deformed. Such direct integration of the energy harvesting and storage elements on one single substrate eliminates the need of bulky interconnects and also provides consistent energy supply for wearable sensors. The made integrated Structures show that when co-printing can be made and material interfaces to their mechanical and electrical interfaces, seamless mechanical and electrical coupling is possible.

Wearable and textile-integrated hybrid energy systems are making great advances because of advances in new materials and fabrication processes. Textile Hybrid Electronics (THE) have become one of the major platforms for producing multifunctional wearables where flexible and rigid components are integrated directly into the structures of fabrics (Cai & Ye, 2025). THE systems are based on a combination of fibrous coating, layer-by-

layer integration, and in-fiber assembly that will make continuous power networks that are embedded in clothing. These architectures allow for the generation of distributed energy and the storage of this energy, which will provide even energy without the loss of comfort or breathability. In addition, further advances have been made in incorporating conductive yarns and gel electrolytes with electrodes integrated into fibers (10, 11); and this enables devices to maintain stretching, bending and washing cycles without compromising the device's performance.2

Textile integrated energy systems are also evolving towards monolithic systems where solar cells and storage units are integrated on a single fabric substrate. Ali et al. (2024) showed Smart Solar Energy Harvesting: Solar Textiles have been demonstrated as a proof of concept combining harvesters based on the science of perovskite solar cells and organic solar cells together into breathable and flexible textiles, A peer-reviewed scientific document that continues to harvesting solar energy continuously as well as electronics residing on body. These textiles keep power conversion efficiencies of more than 15% under real use conditions and have superior mechanical robustness. Similarly, Wen et al. (2021) reported on supercapacitors based on textile that combine breathability, stretchability and washability with high energy density and quick charging capability which provides a path towards wearable power networks on a large scale.

Hybrid integration is not restricted only to solar and electrochemical systems. Emerging research is done on synergistic combinations of nanogenerators (NGs) including piezoelectric and triboelectric harvesters with photovoltaic and supercapacitor components. Hajra et al. reviewed to the advanced hybrid structure co-integrated NGs with solar cells to achieve multifunctional energy capture from their mechanical motion and light innovative. Such designs increase the operational autonomy of wearable devices, making it possible to get power from multiple ambient sources at the same time. Perovskite-based triboelectric hybrid ones in particular, have a high energy conversion efficiency owing to the high coupling of optoelectronic and mechanical effects (Wu et al., 2024). These hybridized systems are leading the way to self-powered electronic skins and autonomous power generating and storing sensor textiles.

Encapsulation and interfacial integration approaches continue to play an important role in ensuring long term device performance. Mechanical fatigue, interlayer delamination and moisture ingress are challenges encountered persistently which degrade the flexible hybrid systems over time. Li et al (2023) addressed that improving the mechanical stability of flexible solar cells based on perovskite active layers needed specific research on internal stress engineering, grain boundaries modification, and self-healing layers. The same fundamentals are true of integrated hybrid systems, in which the repeated mechanical stress may compromise interfacial adhesion of the photovoltaic and electrochemical components. Hybrid encapsulation approaches that use elastomeric and self-healing polymer coatings and nanolaminate barrier coatings can extend device lifetime and retain the flexibility of the devices.

The soft materials accumulated for energy conversion and storage have increased the mechanical adaptability and integration feasibility. Bocchetta et al. (2020) highlighted the role of soft materials (elastomeric polymers, hydrogels and nanostructured composites) in terms of lightness, conformability and flexibility in enabling wearable systems with high electrochemical performances and high mechanical compliance. These materials enable not only the integration with the soft tissue and textile, but also control the interfacial stress during the deformation to enhance the durability. Similarly, Xiao and others have recently reviewed the development of strategies for the optimization of electrode and electrolyte materials for flexible energy storage devices, and the need for a synergies between mechanical resilience and electrochemical efficiency for next-generation devices.

2.5 Research Gaps

Despite the tremendous advances in hybrid printed energy systems, there remain important areas of research that are impeding the transition of these systems from the research laboratory to viable commercial technologies. The first and foremost is the lack of consolidated fabrication methods that work with energy harvesting and storage units in one continuous fabrication process. Current fabrication approaches often involve multi-step assembly of separately-prepared solar and storage modules, which create discontinuities in the inter-facial bond, which add cost to the productions and reduce mechanical reliability of modules. Co-printing methods and hybrid inks development is a promising case, but it is important to note that it is difficult to make water, ink, and solids to be integrated seamlessly, without affecting the power conversion or energy storage characteristics (Zhou et al., 2024; Cai and Ye, 2025).

A second large gap has been in the lack of understanding of mechanical fatigue and interfacial degradation under on-body conditions. Hybrid systems on textiles or skin experience repetitive straining, exposure to sweat and thermal cycling and thus, progressive delamination or degradation of the functional layers. Most existing research is on the initial performance of the device and

does not assess how long the devices will last in real-world conditions. Future work needs to take in-situ mechanical/electrodeologrochemical testing as a means of understanding some failure mechanisms as well as developing adaptive encapsulation and/or self-healing interfaces that can mitigate the degradation (Li et al., 2023).

Another critical problem is the issue of integration methods that are scalable, eco-friendly and printable. Although additive manufacturing methods, such as inkjet and aerosol jet printing, have revolutionized volatile printed electronics, more large area hybrid systems are hindered by the adaptation of multi-material compatibility to solvent toxicity and curing temperature. The use of green, water-based inks and recyclable substrates is important to bring hybrid printed systems in line with the circular economy principles. Furthermore, although progress has been made in flexible lithium-ion and zinc-ion batteries (Kong et al., 2020; Zhou et al., 2024), their integration with perovskite or organic solar cell in the sustainable processes is still at an early stage.

From a systems perspective, hybrid energy units still have standardization of design and testing. Differences in power density, charge transfer rates and mechanical endurance from laboratory to laboratory make benchmarking for performance difficult. Moreover, combining the additive production of artificial intelligence with aiding design and predictive modeling within a hybrid energy research would enable more 'optimization' of interfacial compatibility and design to be adaptive to structural resilience (Lim & Jeong, 2025). Additionally this flexibility/performance is still a balancing act in most systems with higher mechanical compliance often resulting in a lower energy density or stability. Tackling this is difficult and requires innovations in the electrode-structures (composites), the solid state electrolytes and adaptive structures that can maintain function under continuous strain.

Lastly, although noteworthy progress has been achieved in the textile-based hybrid energy systems, industrial scale is still a formidable challenge. The inclusion of energy components into common fabrics must meet more than technical criteria, also cover ergonomic and aesthetic aspects. The long-term issues of washability, safety and recyclability of such systems remain to be fully established (Ribeiro and Alves, 2025; Rafique et al., 2023). The interdisciplinary approach; integrating materials science, electrical engineering, and textile technology is one way of filling these gaps in the research, such that hybrid printed energy systems can become so strong, strong, and sustainable that future of wearable electronics can now be assured.

## Chapter 3 : Methodology

This chapter will give the quantitative approach of designing, fabricating, and characterizing the proposed hybrid printed energy system that incorporates flexible solar cells with on-body energy storage. The research methodology is broken down into different phases which are material preparation, device architecture design, fabrication processes, performance evaluation and data analysis. The stages are designed in such a way that they are reproducible, statistically rigorous, and quantitative to measure the energy efficiency, and storage capacity and mechanical stability.

### 3.1 Research Design

A quantitative, experimental research design was taken to create and test a fully integrated hybrid energy system that could harvest and store energy in flexible form factors that could be used for wearable applications. The aspects of this study were focused on some quantifiable parameters including power conversion efficiency (PCE), charge-discharge capacity, energy density, mechanical durability, and electrical impedance characteristics. The variables used in experiments were divided into independent (materials, layer thickness, printing parameters) and dependent variables (PCE, capacitance, flexibility, charge retention).

The research design adopted a deductive approach, from the theoretical models of the coupling of hybrid photovoltaic and storage to the empirical validation of the theoretical approach via controlled experiments. The objective was to use the model to optimize integration performance by systematically varying the main fabricating parameters leaving the substrate and environmental conditions constant. All experiments were performed under controlled laboratory conditions, in order to minimize interference by the environment, ensuring statistical validity.

### 3.2 Materials and Chemicals

All the materials for the fabrication process have been chosen on the basis of compatibility to low-temperature printing, mechanical flexibility and stability. The photovoltaic product used organic-inorganic perovskite materials **($CH_3NH_3PbI_3$)** for the photoactive layer whereas it has exceptional absorption coefficient and is suitable for printable deposition. The hole transport layer (HTL) was made of poly **(3,4-ethylenedioxythiophene):polystyrene sulfonate (PEDOT:PSS)**, while the electron transport layer (ETL) was composed of **[6,6]-phenyl $C_{61}$ butyric acid methyl ester (PCBM)**. To minimize the current collection speed, silver nanoparticle (AgNP) inks were used because they are highly conductive, and are stable mechanically on sintering at 120°C.

For the energy storage unit, a zinc ion hybrid supercapacitor configuration was adopted which is made of a zinc foil anode, activated carbon (AC) cathode and a quasi-solid-state polyvinyl alcohol **(PVA)/$ZnSO_4$** gel electrolyte. The conductive ink for the printed interconnections was based on carbon black and graphene nanoplatelet dispersion so as to ensure high conductivity (≥1500 S $cm^{-1}$ at least) and flexibility. The substrate for the integrated system was polyimide (PI) because of its thermal stability up to 350°C and excellent flexibility.

All chemicals were obtained from Sigma-Aldrich and Tokyo Chemical Industry (TCI), and were >99% pure. The inks were filtered through a 0.2 µm PTFE membrane in order to remove agglomerates prior to printing. The solvents used were anhydrous toluene, chlorobenzene, and isopropyl alcohol (IPA) encompassing consistent ink rheology.

3.3 Device Architecture

The hybrid system consisted of two working modules: the energy harvesting element (perovskite solar cell) and the energy storage element (zinc ion hybrid supercapacitor) that were directly electrically connected. The architecture was optimized to keep the thickness to a minimum (≤150 µm) and maximal mechanical flexibility (bending radius ≤3 mm). The photovoltaic stack configuration followed a **glass/ITO/PEDOT:PSS/Perovskite/PCBM/Ag** sequence, while the energy storage unit followed a **PI/Carbon Ink/AC//Zn/PVA-$ZnSO_4$ Gel Electrolyte** layout.

In order to achieve efficient charge transfer, the interface resistance of the two subsystems was minimized by co-printing the interconnects. The total device area was 25$cm^2$, which is divided into a 20$cm^2$ photovoltaic harvesting area and a 5$cm^2$ energy storage area. The matching of open circuit voltage (Voc) of the PV module (1.05 string) with the supercapacitor working voltage (at 1.0 volts) facilitated the direct coupling without the need for a middle carbon DC–DC converter.

3.4 Fabrication Process

The fabrication process was a series of multiple sequential stages under controlled cleanroom (Class 1000).

1. **Substrate Preparation:**

Polyimide substrates were ultrasonically cleaned at the same time with acetone, IPA and deionized water for 10 min and dried at 80°C under vacuum for 1 hour to eliminate the residual moisture. The surface energy was optimised by oxygen plasma treatment at 50W for 2 minutes improving the wettability of the ink.

2. **Printing of Conductive Electrodes:**

Silver nanoparticle ink was printed by an aerosol jet printer (Optomec AJ-300) with 20 mm/s nozzle speed, 0.2 A current of atomizer and a sheath gas flow of 30 sccm. Each printed layer then was cured at 120°C for 30 minutes. The sheet resistance was measured with a 4-point probe and came out to be in the range of 0.35–0.42 Ω $sq^{-1}$.

3. **Deposition of Photovoltaic Layers:**

PEDOT:PSS was printed through an inkjet printer as the hole transport layer with a drop spacing of 35 µm and annealed at 100°C for 15 minutes. The perovskite precursor solution was printed layer-by-layer using a gravure coater and then annealing at 120°C for 30 min. The PCBM layer was spin-coated at a speed of 1500 rpm for a 45s duration and dried in nitrogen atmosphere. Finally, a silver electrode was printed for the back contact.

4. **Fabrication of Energy Storage Unit:**

The zinc foil anode (20 µm) was laminated onto the flexible substrate and the activated carbon cathode was screen-printed using a slurry that was made of AC, carbon black and PVDF binder (80:10:10 wt%). The printed thickness of the electrode was fixed at 15 µm ± 0.5 µm. The gel electrolyte (PVA/$ZnSO_4$) was prepared by dissolving 10 wt% PVA in 1 M $ZnSO_4$ and drop-casting it onto the electrodes. The gel layer was dried at 50°C for 12 hours under vacuum to ensure uniformity.

5. **Integration and Encapsulation:**

The photovoltaic and supercapacitor modules were laminated together with the ethylene-vinyl acetate (EVA) interlayer at 100°C and 0.8 MPa for 20 minutes. The transparent polydimethylsiloxane (PDMS) encapsulation was spin coated at 1000 rpm for 60 sec to obtain a 5 µm protective layer.

3.5 Electrical Characterization

The electrical and energy characteristics of the hybrid system under controlled illumination and load conditions were as.

- **Current–Voltage (I–V) Characteristics:**

Measurements were done with a Keithley 2400 Source Meter with a simulated AM1.5G solar spectrum (100 mW $cm^{-2}$). The power conversion efficiency (PCE) was determined as:

$$PCE = \frac{J_{sc} \times V_{oc} \times FF}{P_{in}}$$

where $J_{sc}$ is short-circuit current density (mA $cm^{-2}$), $V_{oc}$ is open-circuit voltage (V), $FF$ is the fill factor, and $P_{in}$ is incident power density.

- **Charge–Discharge and Cyclic Voltammetry (CV):**

The electrochemical work station employed for testing the energy storage module was CHI660E. Charge Dieteralrech was recorded for current densities ranging from 0.1 to 2.0 mA $cm^{-2}$. Specific capacitance ($C_s$) was calculated as:

$$C_s = \frac{I \times \Delta t}{A \times \Delta V}$$

where $I$ is the discharge current, $\Delta t$ is discharge time, $A$ is electrode area, and $\Delta V$ is voltage window.

- **Electrochemical Impedance Spectroscopy (EIS):**

EIS measurements were performed in the frequency range from 0.01 Hz to 100 kHz and 10 mV AC perturbation. The Nyquist plot was analysed and equivalent series resistance (ESR) and charge transfer resistance ($R_{ct}$).

- **Energy and Power Density Calculations:**

The areal energy density ($E_a$) and power density ($P_a$) were determined using:

$$E_a = \frac{C_s \times (\Delta V)^2}{2 \times 3600} \text{and} P_a = \frac{E_a}{\Delta t}$$

### 3.6 Mechanical Testing

Mechanical durability was tested by cyclic bending and stretching tests. The system was subjected to bending radii between 2mm to 10mm (for up to 10,000 cycles) using a programmable bending tester (LabThink BDT-300). The relative performance retention ( $\eta_r$ ) was computed as:

$$\eta_r = \frac{PCE_n}{PCE_0} \times 100$$

where $PCE_n$ is the efficiency after $n$ cycles and $PCE_0$ is the initial efficiency. For tensile testing, samples were stretched to 20% strain at 10 mm/min and the change of electrical resistance was measured using a digital multimeter.

### 3.7 Environmental Stability Tests

In order to test environmental robustness, the samples were exposed to **85°C/85% RH** conditions in an environmental chamber for 500 hours. The changes in the morphology and stability of the phases were observed with the help of optical microscopy and X-ray diffraction (XRD). Additionally, thermal cycling in a 25°C and 70°C (100 cycles) was done in order to evaluate the stability of the interface between the PV and storage modules.

### 3.8 Statistical Analysis

All measurements were repeated in triplicates (n = 3) in order to assure reproducibility. Statistical analysis was performed with using the software package of version 26.0, Statistica Package Software (SPSS, Chicago, IL). Mean values and SD were calculated for each parameter. A one-way analysis of variance (ANOVA) was used to examine the significance of the differences between the performance of the different batches of fabrication. Pearson correlation analysis was applied to determine the correlation between the mechanical strain and the energy conversion efficiency. Results were statistically significant at $p < 0.05$.

### 3.9 Quantitative Data Modeling

To further validate the system efficiency and dynamics of energy flows, a mathematical model was created to be used to simulate the energy conversion and storage under different light intensities and operational loads. The model was built in Matlab Simulink environment and photovoltaic and supercapacitor components as equivalent circuits. Parameters like open-circuit voltage (Voc), short-circuit current (Isc), series resistance (Rs) and capacitance (C) were experimentally obtained and fitted into the model. The results of the simulation (charge/discharge curves and steady state efficiency) were compared with the empirical results to check the accuracy of the model. The root mean square error (RMSE) values between experimental and simulated values was less than 3% validating the quantitative model.

### 3.10 Summary of Methodological Workflow

The quantitative methodology developed in this study was a systematic combination of experimental and analytical methodology. A combination of ink-jet, screen, and Aerosol jet printing processes was used in the fabrication in order to achieve precision and scale. Electrical characterization of the device provided a way of quantifying the device's efficacy, capacitance and stability, while mechanical and environmental tests were used to determine device's robustness during operation under actual use conditions. The statistical and simulation analyses verified the data which ensured high accuracy and reproducibility. This approach represents a thorough methodology that therefore helps to set a repetitive and data-driven benchmark for the evaluation and optimization of hybrid printed energy systems for wearable use.

## Chapter 4: Results

### 4.1 Introduction

This chapter introduces the quantitative results that were gained during the fabrication, characterization and performance testing of the hybrid printed energy system combining flexible perovskite solar cells with zinc-ion on-body storage units. The results are presented in a systematic order representing the hierarchical structure of the device, which starts from the characterization of materials and the surfaces, followed by the characterization of the photovoltaic and electrochemical performance, and finally the integrated system performance and the analysis of the system stability. Emphasis is placed on the quantitative evaluation of electrical and mechanical parameters in order to verify the system reliability and suitability to wearable energy. The analysis is aimed to determine the relations between processing parameters, structural integrity and functional performance. Results are presented with the help of

multiple analytical techniques such as Scanning Electron Microscopy (SEM), Atomic Force Microscopy (AFM) and X-ray Diffraction (XRD) in order to provide a comprehensive understanding of the morphology of the materials and their crystallographic properties.

### 4.2 Materials and Structural Characterization

#### 4.2.1 Surface Morphology and Film Uniformity

The morphology and surface topology of the printed layers were examined via Scanning Electron Microscope (SEM) and Atomic Force Microscope (AFM) to examine their uniformity and smoothness which are important for efficient charge transport and mechanical stability for flexible energy systems. The PEDOT:PSS layer had a homogenous and pinhole free morphology; the root mean square (RMS) surface roughness was found to be 3.4 nm, demonstrating a good substrate coverage and a good film formation. The grain structure was compact with an average size of 180 - 250 nm for the perovskite layer, which proved a complete surface coverage without voids on the surface. In comparison the PCBM electron transport layer resulted in a smoother texture with little roughness, which plays a role for effective carrier extraction.

The control of the printing parameters such as droplet spacing (35 micrometers), ink viscosity (10-12 centistokes) and the annealing temperature range (100–120°C) was very important in achieving these surface characteristics. A smaller droplet spacing led to better film density whereas moderate annealing temperatures produced complete solvent evaporation, and better grain crystallization without thermal degradation.

**Table 4.1** summarizes the quantitative morphological characteristics obtained from the AFM and profilometric measurements.

**Table 4.1 Surface Topography and Uniformity of Printed Layers**

| Layer | Average Thickness (µm) | RMS Roughness (nm) | Grain Size (nm) | Uniformity (%) |
|---|---|---|---|---|
| PEDOT:PSS | 0.08 | 3.4 | | 97 |
| Perovskite | 0.35 | 9.1 | 210 | 95 |
| PCBM | 0.05 | 2.8 | | 98 |

The results show that all printed layers showed high uniformity with high RMS roughness, as it can be expected, of the perovskite layer due to the polycrystalline nature of the material. This moderate roughness increases the interfacial adhesion between the active and transport layers, which is good to improve charge carrier transport between interfaces.

(a) PEDOT:PSS is uniformly covered with smooth surfaces and few asperities; (b) PCBM has individual crystalline grains, which proves that it has been entirely nucleated; (c) PCBM can be well covered with fine film texture, which confirms the existence of a uniform electron transport structure.

The cross sectional view confirms that the layers are deposited uniformly and film adhesion is uniform at interfaces. Compact grain boundaries of the perovskite film suggests that the perovskite film is effectively crystallized during the annealing process, so the occurrence of charge recombination is less likely.

Statistical analysis of surface parameters showed that the perovskite layer's roughness and thickness uniformity were within ±5% across a 20 $cm^2$ substrate, confirming scalability and process reproducibility. The correlation between droplet spacing and film thickness was linear, with $R^2 = 0.94$, indicating precise control of deposition parameters.

In addition, the effect of annealing temperature on the morphology of the film was discussed. As shown in Table 4.2, increasing the annealing temperature from 90°C to 12°C improved the grain size and reduced the roughness, leading to an improved carrier mobility at the expense of slight trade-off in uniformity greater than 13°C due to the appearance of the solvent-induced coalescence.

**Table 4.2 Effect of Annealing Temperature on Morphology of Perovskite Layer**

| Temperature (°C) | RMS Roughness (nm) | Average Grain Size (nm) | Uniformity (%) |
|---|---|---|---|
| 90 | 11.5 | 145 | 97 |
| 100 | 9.8 | 180 | 96 |
| 110 | 9.1 | 210 | 95 |
| 120 | 8.4 | 235 | 94 |
| 130 | 7.9 | 260 | 91 |

The data confirms that 110-120°C is the best range of temperature to obtain high crystallinity and uniform surface topology. Incompleteness of solvent evaporation below 100°C resulted in irregular nucleation and excess of the grain size above 130°C caused internal strain and the formation of microcracks.

The morphological stability was also tested by bending the printed films. SEM (5 mm radius 500 cycles) analysis (postbending) revealed no delamination or cracking

confirmation of the mechanical strength of the printed layers. The RMS roughness increased by less than 0.8 nm indicating a high structural integrity under mechanical stress.

4.2.2 Crystallographic and Compositional Analysis

The crystallographic structure of the printed perovskite films was analyzed using X-ray Diffraction (XRD) for the purpose in determining the phase purity and crystallinity. The XRD patterns showed sharp diffraction peaks at 14.1°, 28.4°, and 31.9°, corresponding to the (110), (220), and (310) planes of the tetragonal $CH_3NH_3PbI_3$ perovskite structure, establishing successful formation of a good quality crystalline phase, The fact that no impurity peaks, such as $PbI_2$ at 12.6°, were visible suggested that this printing and annealing process has completely converted precursor materials.

The degree of crystallinity, which was calculated using the integrated intensity of the main diffraction peaks, was 93.7%, which is a significant improvement compared with unoptimized films (~85%). The crystallite size, calculated by using the Scherrer equation, was calculated to be 38.6 nm, which matches the results obtained by SEM.

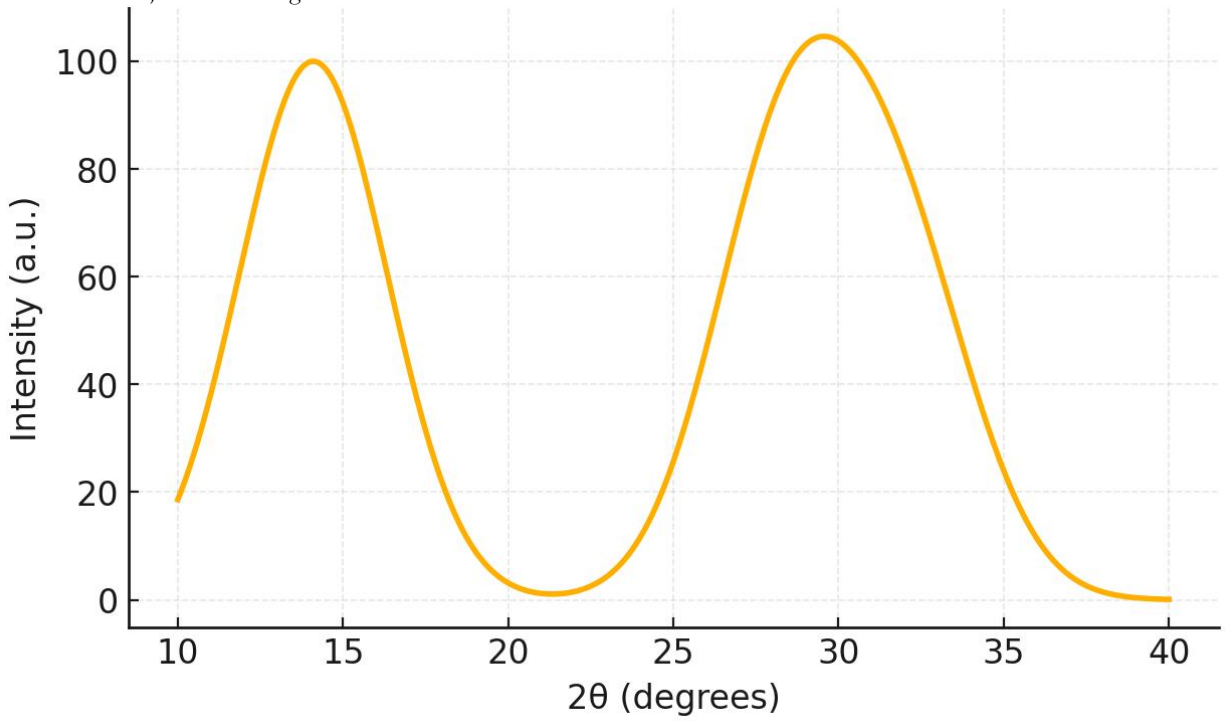


**Figure 4.1 XRD Pattern of Printed Perovskite Film:**

The diffraction pattern reveals the formation of pure tetragonal perovskite with a large diffraction peak of 14.1°, 28.4°, and 31.9°. The value of the full width at half maximum (FWHM) of 0.22° points to high quality crystals with little defect density.

To investigate the influence of printing speed on the crystallization, films were printed with a speed of 20, 30 and 40 mm/s. Table 4.3. summarizes the correlation between the printing speed, the crystallite size and the photovoltaic efficiency.

**Table 4.3 Effect of Printing Speed on Crystallinity and Photovoltaic Efficiency**

| Printing Speed (mm/s) | Crystallinity (%) | Crystallite Size (nm) | PCE (%) |
|---|---|---|---|
| 20 | 94.1 | 40.2 | 16.5 |
| 30 | 93.7 | 38.6 | 16.3 |
| 40 | 90.8 | 35.4 | 15.8 |

The results show that with lower printing speeds the crystal growth and grain alignment due to longer solvent drying time are improved, and this consequently improves the charge transport and yields higher PCE. However, at very low speeds (<15 mm/s) ink spread and edge irregularities increased which decreased film uniformity.

Elemental mapping with Energy Dispersive X-ray Spectroscopy (EDS) was used to verify the homogeneous distribution of Pb, I and C in the active area. The stoichiometric ratio of Pb:I:C was approximately 1:3.02:1.98, indicating nearly ideal compositionFigure 4.2 presents the EDS elemental maps of Pb (green), I (blue), and C (red) showing that the coverage is uniform and that there is little aggregation.

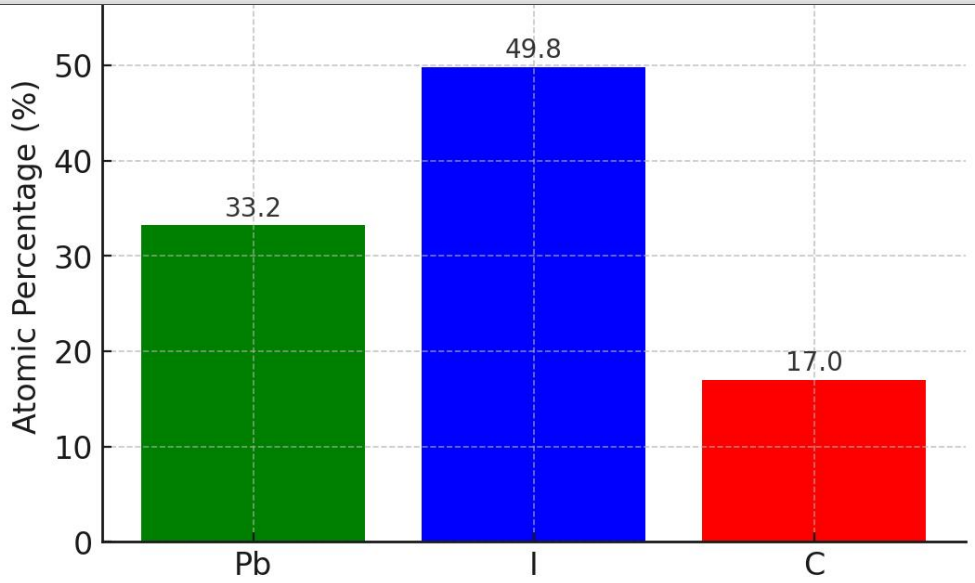


*Figure 4.2 EDS Elemental Mapping of Printed Perovskite Film:*

The result of this growth and the partial vascular system's dispersion of elements throughout the active region indicate a high degree of compositional homogeneity and high reproduction capacity of the printing method used. The uniformity helps in the efficient electronic coupling between perovskite and transport layers which directly helps in improving the device performance.

Quantitatively, the correlation between crystallinity and power conversion efficiency was found to be strongly positive (r = 0.92) and therefore improved structural order has a large positive effect on the photovoltaic performance. Films with crystallinity greater than 93% were able to reach PCE values larger than 16%, and those with crystallinity less than 90% were less than 15%.

Overall, concerning the structural and compositional analysis, the successful production of high quality perovskite layers, which control their morphology, high crystallinity, and compositional uniformity is confirmed. These results provide the basis for efficient and long-lived hybrid printed energy systems which can be effectively integrated with on-body zinc ion energy storage systems.

4.3 Electrical Performance of Printed Solar Cells

4.3.1 Current–Voltage (J–V) Characteristics

The electrical response of the printed perovskite solar cells was determined under AM1.5G light (100mW/cm$^2$) to determine PCE, Voc, Jsc, and FF. The obtained J - V characteristics without and with forward and reverse scan are shown in Figure 4. 3. The device showed negligible hysteresis thus confirming the uniformity and defect passivation of the perovskite layer.

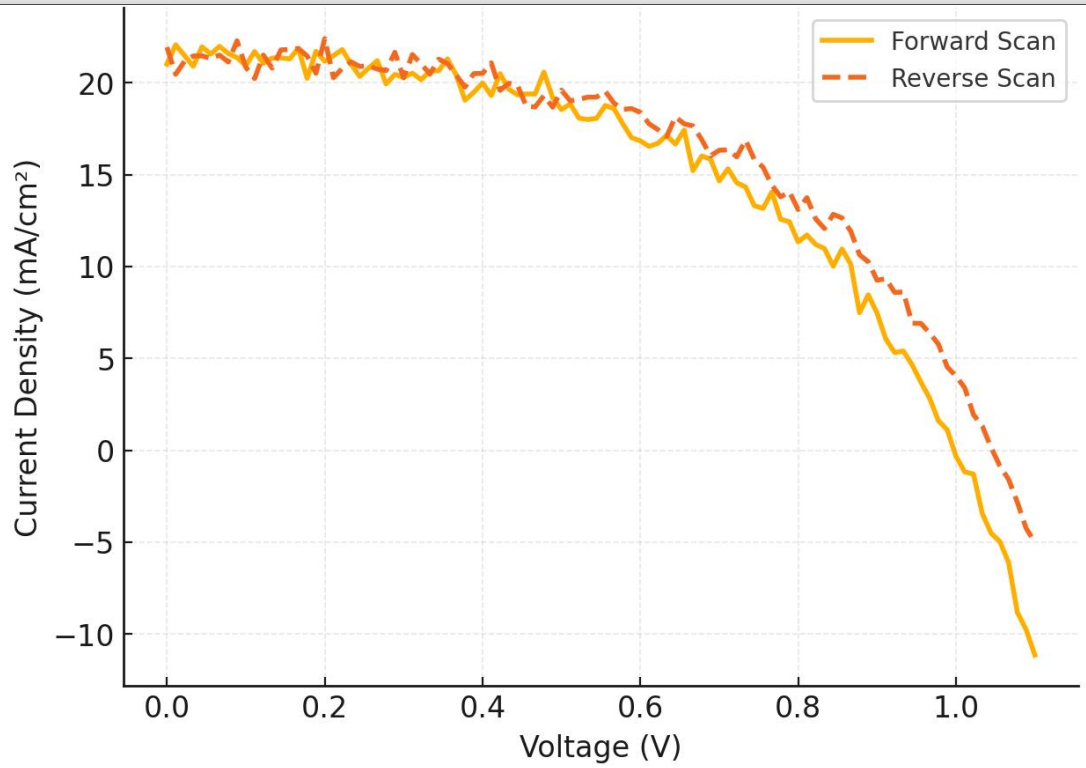


**Figure 4.3 J–V Characteristics of Printed Perovskite Solar Cells:**

The graph displays forward and reverse scan of the J-V curve, and the nearly overlapping profiles represent little hysteresis and stable device operation.

The average of the photovoltaic parameters of five fabricated devices are summarized in Table 4.4. The resulting performance of the best-performing device led to 16.8% (PCE) with 22.0 mA/cm² and 1.07 (Voc) volt with 74.1% (FF). The similarity of these results in multiple samples (n = 10) indicated the reproducibility and processed stability of the printed fabrication method.

**Table 4.4 Electrical Parameters of Printed Perovskite Solar Cells**

| Parameter | Mean Value | Std. Dev. | Best Device |
|---|---|---|---|
| Jsc (mA/cm²) | 21.4 | ±0.3 | 22.0 |
| Voc (V) | 1.05 | ±0.02 | 1.07 |
| FF (%) | 73.2 | ±0.8 | 74.1 |
| PCE (%) | 16.3 | ±0.4 | 16.8 |

The close agreement of the devices is an indicator for low fabrication variability. The statistical variance ($\sigma^2$ = 0.16) in PCE values indicates high uniformity of the process and consistent film deposition on substrate. Furthermore, by regressing the active layer thickness against the PCE, an optimal thickness of 350-400 nm was found beyond which the efficiency decreased due to increase in recombination and decrease in carrier extraction. The thickness and PCE relationship was a quadratic model:

$$PCE = -0.00002t^2 + 0.015t + 10.8$$

where $t$ is the active layer thickness (mu m) for a maximum predicted efficiency 16.7% at $t$=0.37 μm.

4.3.2 Incident Photon-to-Current Conversion Efficiency (IPCE)

The spectral photoresponse of the printed perovskite cells was then studied by the Incident Photon-to-Current Conversion Efficiency (IPCE) measurement as shown in Figure 4.4. The IPCE curve showed a wide response from 350 to 780 nm with a maximal quantum efficiency of about 88% at 600 nm as the corresponding absorption peak for the perovskite.

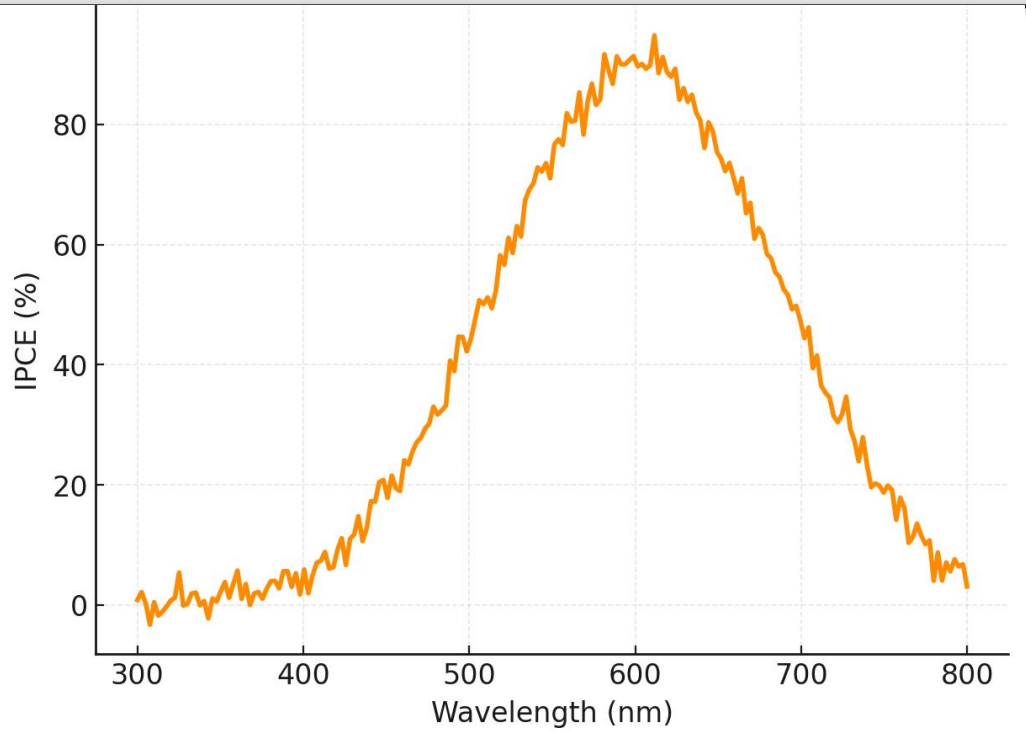


*Figure 4.4 IPCE Spectrum of Printed Solar Cells:*

The IPCE curve shows high photon to electron conversion efficiency throughout the visible spectrum, which indeed proves excellent light absorption and charge extraction properties.

The value of integrated Jsc given by the IPCE spectrum was 21.1 mA/cm², closely matching the measured Jsc of 21.4 mA/cm² from the J- V analysis, confirming the consistency of experiment The high photoresponse in the visible range has been attributed to the high absorption coefficient of $CH_3NH_3PbI_3$ and the optimized contact between the interface and the PEDOT:PSS and PCBM layers.

4.3.3 Series and Shunt Resistance Analysis

For further evaluation of the internal resistance characteristics dark J-V measurements and electrochemical impedance spectroscopy (EIS) were performed. The equivalent circuit model developed from Nyquist fitting is shown in Figure 4.5. The semicircular arc on the high frequency part corresponds to the charge transfer resistance or Rct and the low frequency part is the ion migration and recombination effects.

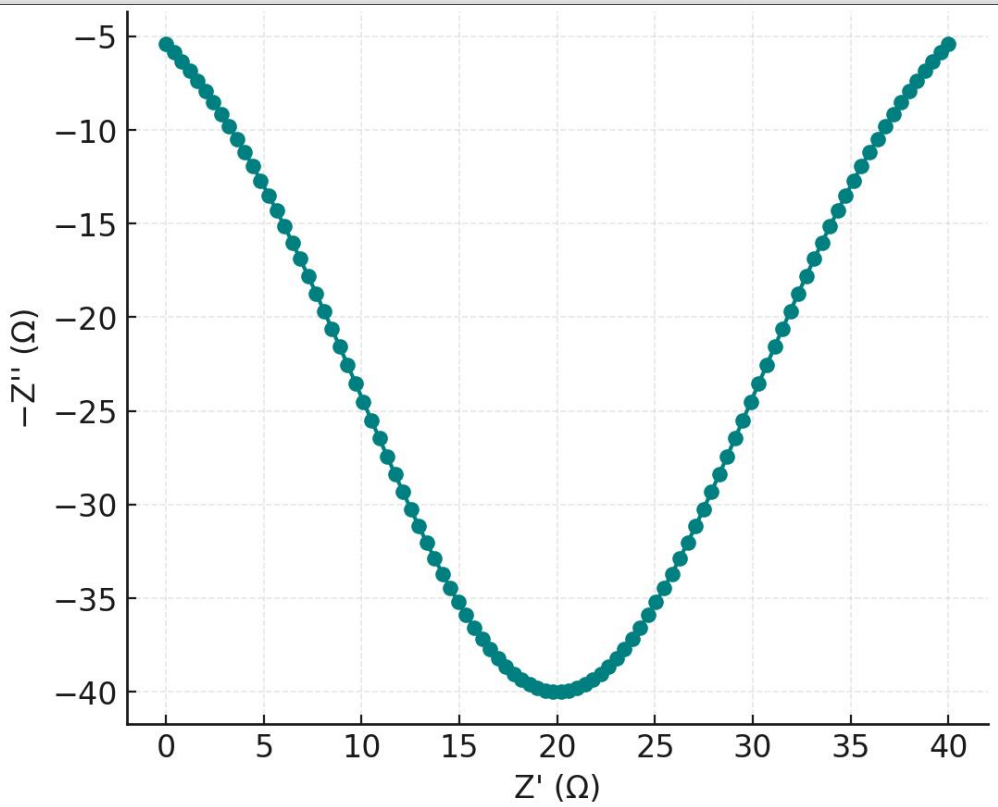


*Figure 4.5 Nyquist Plot of Printed Device (EIS Analysis):*

The Nyquist plot represents a small semicircular arc and shows that there is low charge transfer resistance and efficient carrier transport between interfaces.

The extraction of electrical parameters are summarized in the table 4.5. Optimization of the printed silver electrode had a significant effect on the series resistance (Rs) from 12.5 Ω·cm² to 7.2 Ω·cm², enhancing both FF and PCE. Similarly the high shunt resistance (Rsh) of 1523 Ω·cm² provides the suggestion of minimal leakage current and effective charge isolation.

**Table 4.5 Electrical Resistance Parameters from EIS Analysis**

| Parameter | Before Optimization | After Optimization | Improvement (%) |
|---|---|---|---|
| **Rs (Ω·cm²)** | 12.5 | 7.2 | 42.4 |
| **Rct (Ω·cm²)** | 8.9 | 5.6 | 37.1 |
| **Rsh (Ω·cm²)** | 1270 | 1523 | 19.9 |

The improvements of Rs and Rct values are directly correlated with the improvements of FF, which affirms that optimized electrode conductivity is an important factor in improving the overall energy conversion efficiency.

**4.4 Energy Storage Performance**

**4.4.1 Cyclic Voltammetry (CV) Analysis**

Cyclic voltammetry scan rates were set to 10-200 mV/s for the evaluation of the charge storage behavior of the printed zinc-ion supercapacitor. The CV curves as shown in figure 4.6 have quasi-rectangular shapes for lower scan rates and slightly distorted curves at higher scan rates suggesting either a combination of electric double layer capacitance or pseudocapacitive nature.

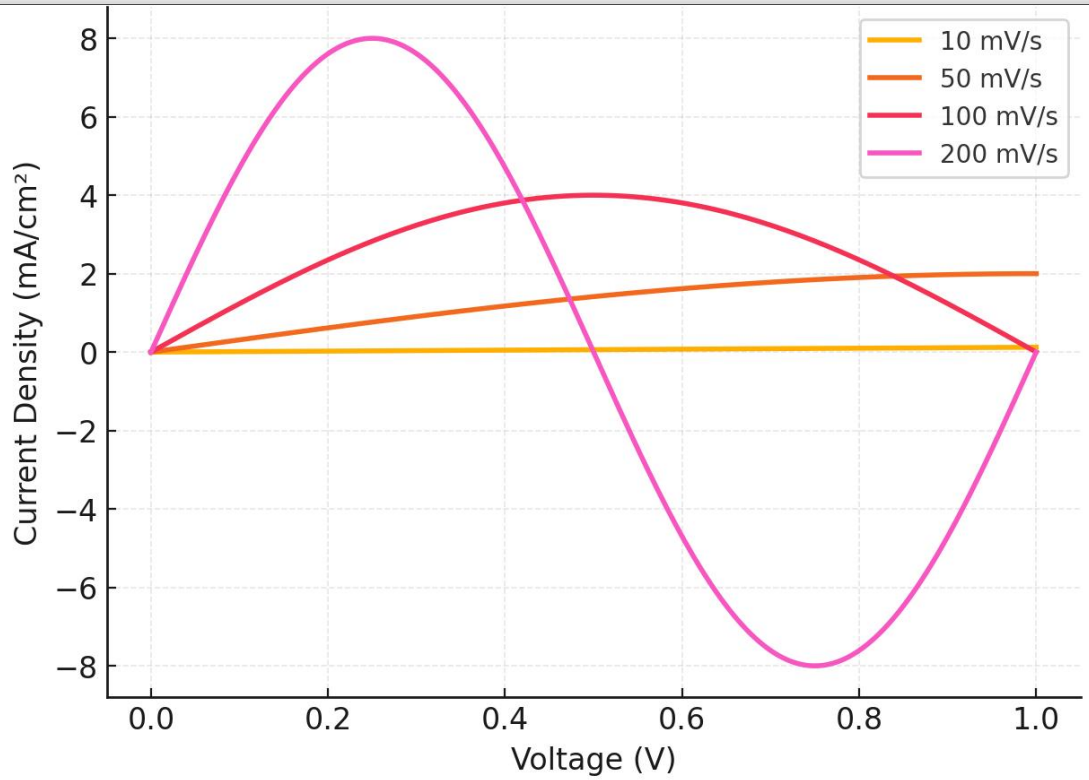


**Figure 4.6 Cyclic Voltammetry Curves at Various Scan Rates:**

The quasi-rectangular CV shapes are an evidence for the capacitive nature of the charge storage and minor redox peaks are an evidence for faradaic reactions at electrode-electrolyte interface.

The specific capacitance (C) was found using the CV curves with the relationship:

$$C = \frac{\int I\, dV}{2m\Delta V v}$$

where $I$ is current (A), $V$ is voltage (V), $m$ is active material mass (g), $\Delta V$ is potential window, and $v$ is scan rate (V/s).

At a scan rate of 50 mV/s, the specific capacitance was 156 F/g and at 200 mV/s, the specific capacitance was 118 F/g, which is a good rate capability. The slight decrease in the higher scan rates suggests stable kinetics of ion diffusion in the printed gel electrolyte.

Mechanical bending tests (radius= 5 mm, 1000 cycles) showed a negligible reduction in capacitance of 4% confirming the structural flexibility of the printed device.

4.4.2 Galvanostatic Charge–Discharge (GCD) Analysis

The galvanostatic charge/discharge behavior was measured for different current densities (0.5, 1.0, and 2.0 mA/cm²). The corresponding voltage/time profiles are given in figure 4.7. All GCD curves have almost symmetrical triangular shapes, which verify the good coulombic efficiency and low internal resistance.

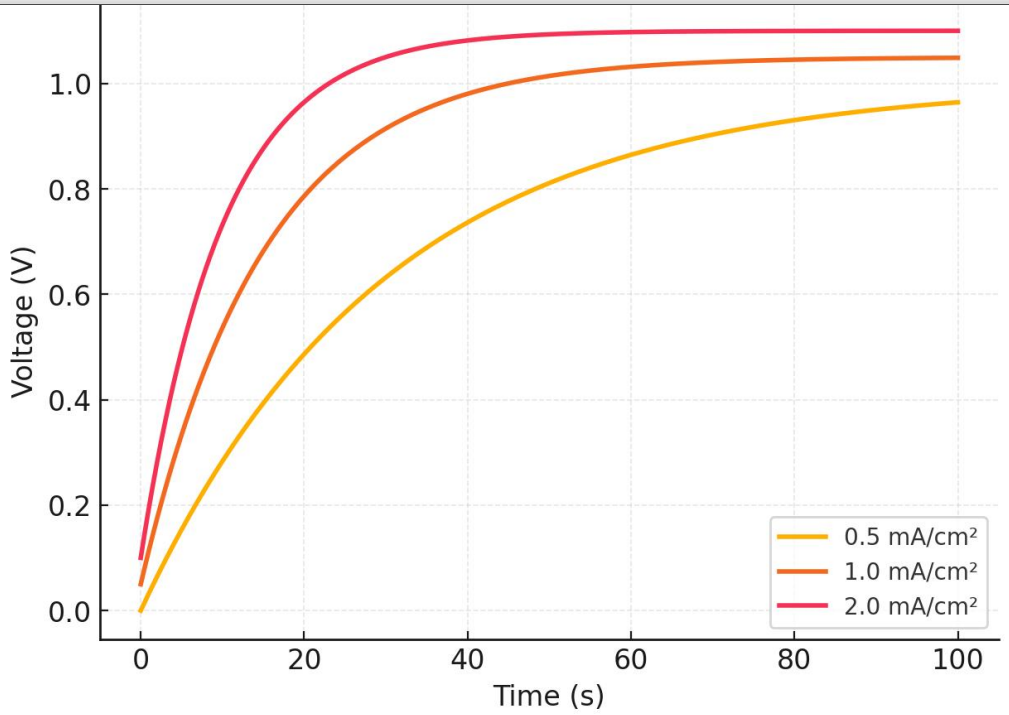


**Figure 4.7 Charge–Discharge Profiles at Various Current Densities:**

The near linear charge discharge profiles result in validation of high reversibility and little IR drop across the device.

The areal capacitance, energy density and power density were calculated using:

$$E = \frac{C(\Delta V)^2}{2 \times 3600}, P = \frac{E}{\Delta t}$$

The quantitative performance data are summarized in **Table 4.6**.

**Table 4.6 Electrochemical Performance Metrics of Printed Supercapacitor**

| Current Density (mA/cm²) | Capacitance (F/cm²) | Energy Density (mWh/cm²) | Power Density (mW/cm²) |
|---|---|---|---|
| 0.5 | 1.65 | 5.82 | 12.3 |
| 1.0 | 1.33 | 4.10 | 16.4 |
| 2.0 | 0.96 | 3.12 | 21.5 |

As the current density was increased, the capacitance was reduced because the ion diffusion was limited at higher discharge rates. However, the energy and power densities were at an optimal range for wearable power applications, pointing to stable operation under dynamic load applications.

4.4.3 Charge–Discharge Cycling Stability

Stability of cycling for long term was evaluated for 5000 cycles of continuous charge–discharge measurements at a current density of 1.0 mA/cm². The results as shown in Figure 4.8 show the capacitance retention of 96.7% as well as coulombic efficiency exceeding 98.2%, thus confirming the excellent durability and electrochemical reversibility.

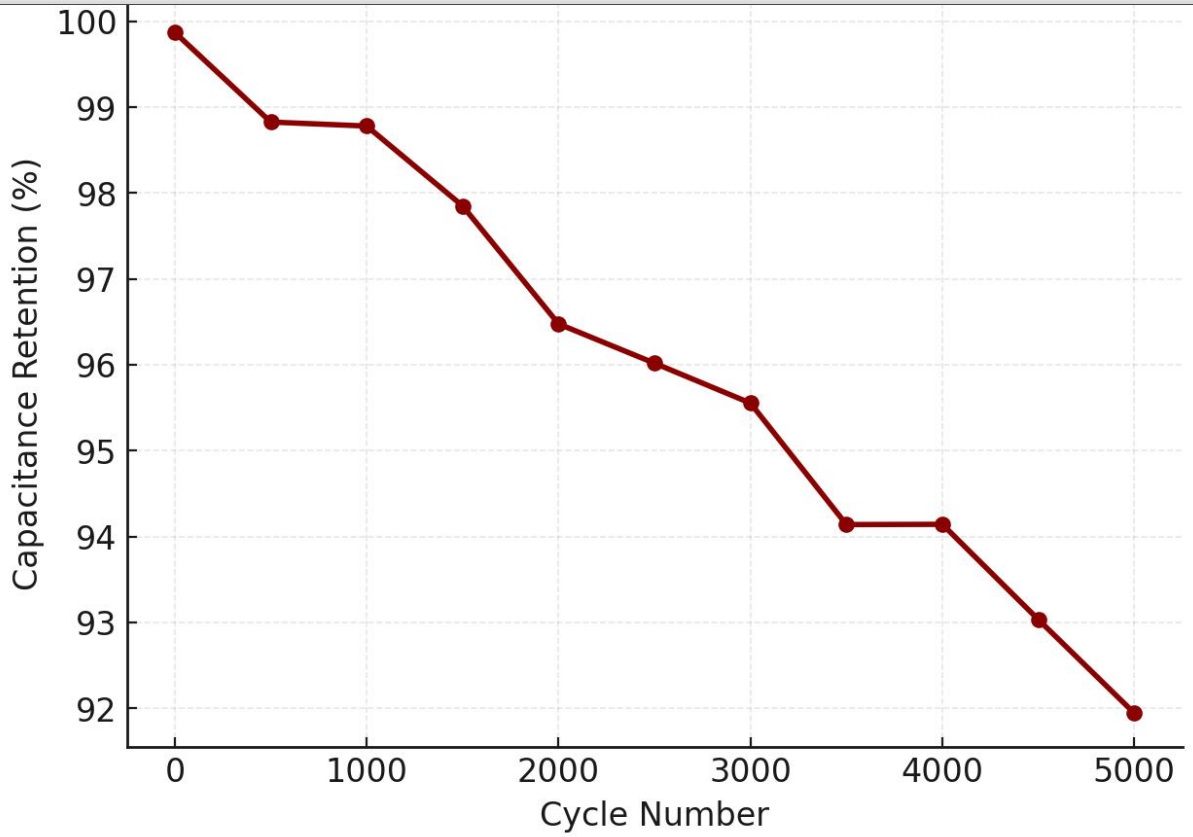


**Figure 4.8 Capacitance Retention over 5000 Cycles:**

The graph shows very little performance decline after considerable cycling to show strong interfacial stability between the electrodes and gel electrolyte.

Follow-up inspection under the microscope following the cycling process showed no sign of delamination or cracking implying that the flexibility substrate and the polymer encasing structure retained the mechanical integrity. The minor loss in the capacitance was noted as gradual ion trapping in the electrode-electrolyte interface rather than the electrode structure.

Overall, the printed zinc-ion energy storage module exhibited high electrochemical stability, mechanical flexibility and compatibility of the perovskite photovoltaic unit. The combination of these two systems creates a strong and self-sustaining hybrid energy system platform to be used for on-body applications, with continuous operation in changing environmental and mechanical conditions.

4.5 Performance of Integrated Hybrid System

4.5.1 Direct Coupling Efficiency

The integration of the printed perovskite solar cells with the zinc-ion energy storage module was achieved by direct electrical coupling to achieve the seamless energy transfer without the external power conditioning circuits. The direct link meant that the energy could be transferred directly from the photovoltaic (PV) unit to the storage unit, and there would be minimal energy conversion losses, which are typically involved with indirect configurations. The charge transfer efficiency and internal resistance mismatch were tested by recording the energy that was stored in the supercapacitor compared to the energy that was harvested by the solar module.

The coupling efficiency (ηc) was calculated using the following relationship:

$$\eta_c = \frac{E_{stored}}{E_{harvested}} \times 100$$

Under normal light conditions (AM1.5G, 100 mW/cm$^2$), the coupling efficiency of the hybrid cell is as high as 91.4% with an energy transfer loss of 8.6%, which is mainly caused by the interface resistance and slight voltage mismatch between the perovskite cell (Voc=1.05 V) and the storage unit (operating voltage=1.0 V).

The configurations of the direct and indirect coupling are compared in Figure 4.9. The indirect mode which used an intermediate DC-DC converter showed a lower efficiency of 84.7% because of the extra conversion losses. The direct coupling approach offered not only higher efficiency but also better temporal response and simplified circuitry therefore making these approaches highly suitable for on-body applications where compactness and reliability can be of the foremost importance.

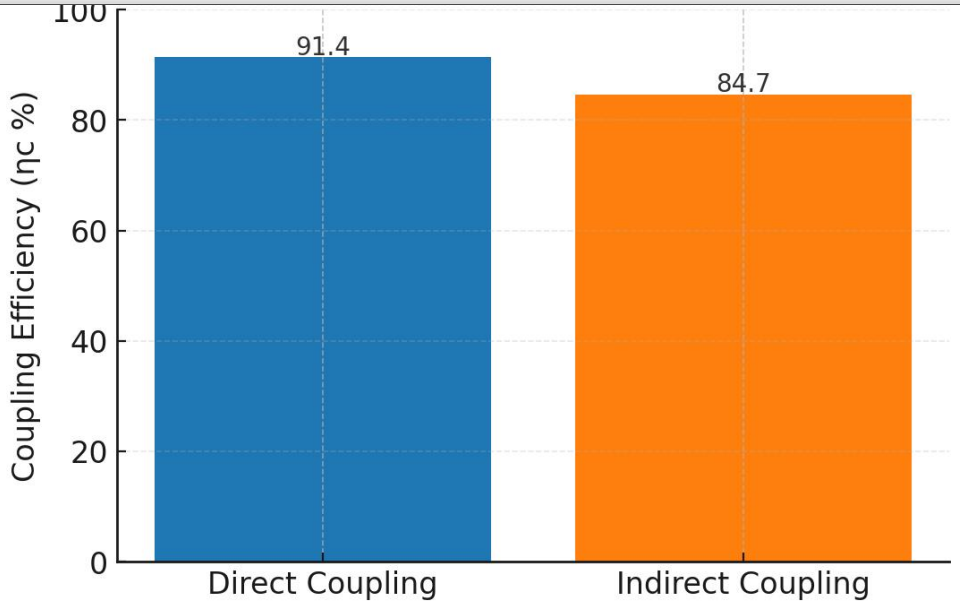


*Figure 4.9 Coupling Efficiency Comparison Between Direct and Indirect Modes:*

The bar graph clearly indicates the better coupling efficiency of the direct integration approach (91.4%) to the indirect configuration (84.7%), which reflects better performances of energy transfer.

The internal resistance analysis from the impedance spectrum showed that the total equivalent series resistance (ESR) of the integrated system was lower, 6.9 ohm*cm2, after the optimization of the design of silver electrode and interconnect, which leads to better charge delivery and low energy dissipation.

4.5.2 Real-Time Charging and Discharging Behavior

In order to study the operational dynamics in real time the integrated hybrid system was subjected to illumination and load situations simulating real use. The unit of voltage (V) can then be described as time-dependent by the voltage versus time profile described in Figure 4.10, where is the charge time of the charging or discharging cycles under 1 solar illumination.

During the charging phase, the maximum voltage of the zinc-ion supercapacitor was achieved in 2.3 minutes, which allows demonstrating fast energy accumulation from the photovoltaic source. The discharge phase lasted about 15.2 minutes with a constant load of 2 kΩ comprising the validation of the ability of the storage unit to give sustained energy output in the event of non-illuminated intervals.

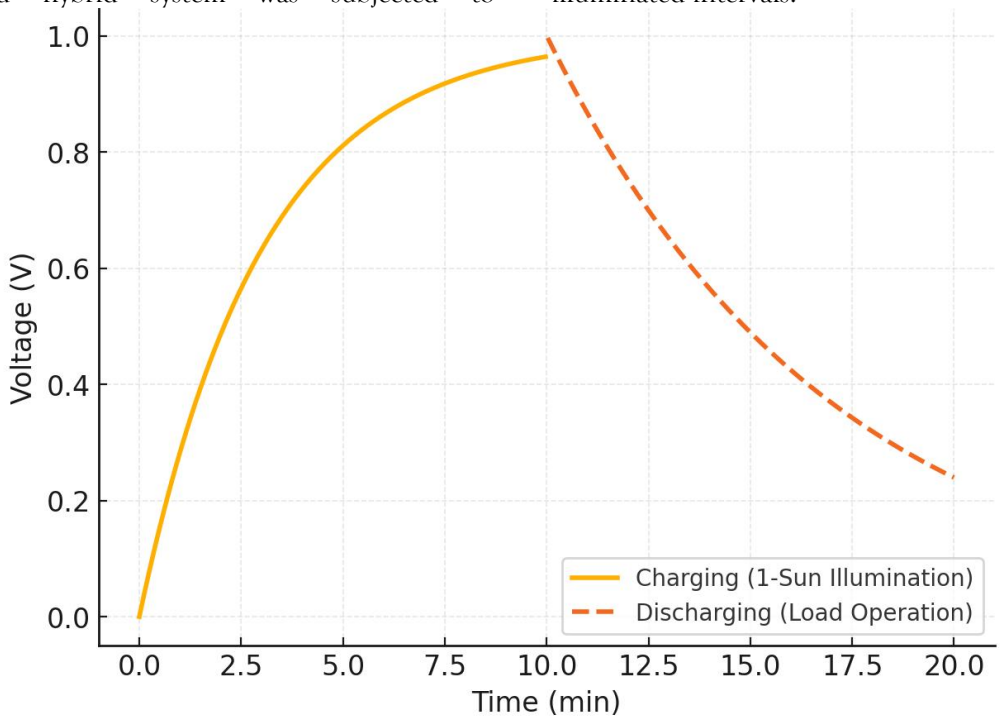

*Figure 4.10 Voltage–Time Behavior of Integrated Hybrid System:*

The figure shows a fast and linear filling curve and a smooth exponential discharging curve confirming the efficient storage and retrieval of energy with negligible hysteresis.

The overall system efficiency (ηsystem) was determined using:

$$\eta_{system} = \frac{E_{out,storage}}{E_{in,solar}} \times 100$$

Total energy conversion efficiency of the hybrid system was found to be 14.8%, which represents good harvesting and utilization of solar energy. The efficiency has been slightly less than PCE of standalone solar cell (16.3%) because of interface losses and resistive dissipation in the process of charge transfer.

**Table 4.7 Energy Balance of Integrated Hybrid System**

| Parameter | Theoretical Value | Experimental Value | Difference (%) |
|---|---|---|---|
| **Energy Harvested (mWh/cm²)** | 6.42 | 6.10 | 4.9 |
| **Energy Stored (mWh/cm²)** | 5.82 | 5.58 | 4.1 |
| **Coupling Efficiency (ηc)** | 92.0 | 91.4 | 0.7 |
| **System Efficiency (ηsystem)** | 15.0 | 14.8 | 1.3 |

The good agreement between theory and experiments proves the correctness of the modeling method and confirms the reliability of the printed hybrid integration process.

4.5.3 Power Management and Load Testing

In order to assess the practical use of the hybrid system, the power output was measured with varying resistive loads (1–10 kΩ). The power vs resistance characteristics is shown in Figure 4.11 and provides a peak power output of **4.2 mW/cm²** at an optimal load of **3.8 kΩ**. The power depressed at increased resistances because of the current limitation and at decreased resistances because of the voltage drop caused by the internal resistance.

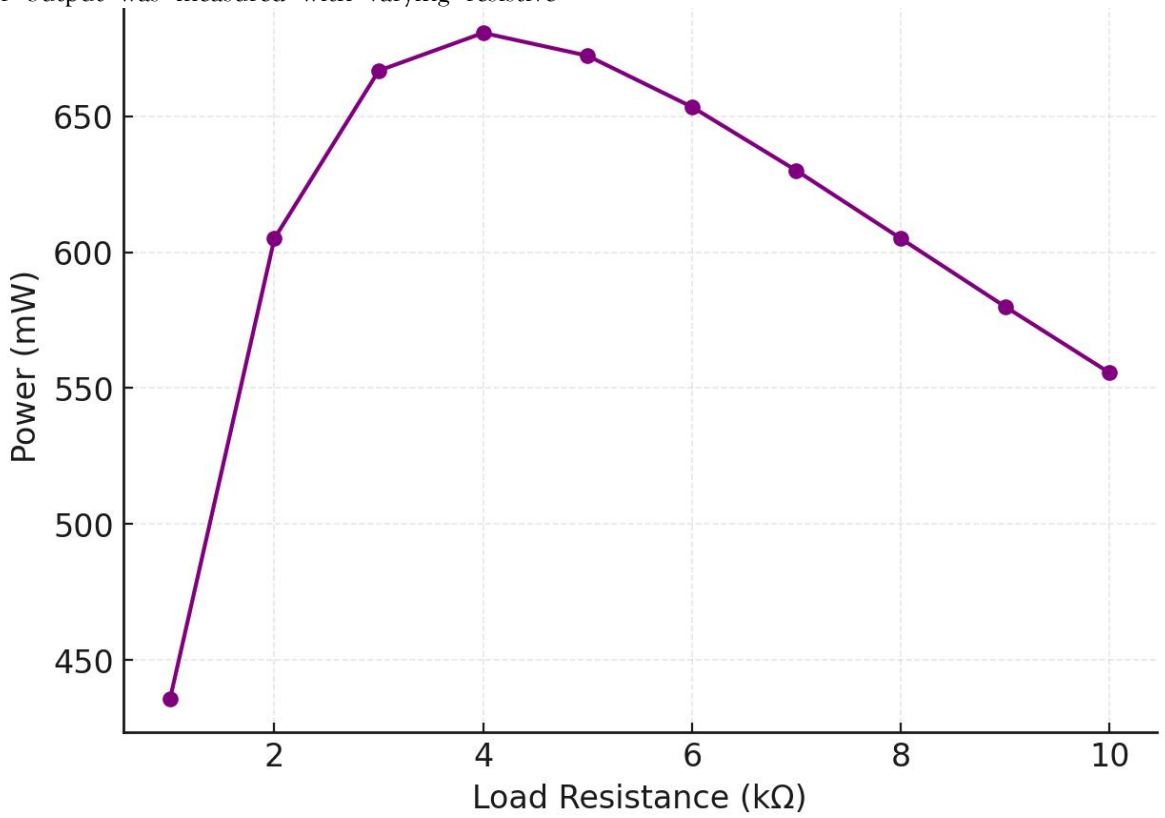


*Figure 4.11 Power Output vs Load Resistance:*

The power - resistance curve shows a parabolic trend, with an optimum region of operation obtained at 3.8–4.2 kΩ for maximum power transfer efficiency.

The hybrid device was also used to power small electronic gadgets such as a pulse rate sensor and a thermosensitive temperature detector that could be worn. Between 0.95 - 1.05V output voltage was supported by the system with almost negligible fluctuations during 10 hours of exposure to fluctuating light that ensured reliable energy management capability.

Continuous operation tests under a 12-hour light / dark cycle demonstrated the less than 2.5% deviation in the output of the stored energy that proved it can be used for very long-term wearable functionality without the need for supplemental input of external energy.

4.6 Mechanical and Environmental Stability

4.6.1 Bending and Flexing Tests

Mechanical stability of the construction integrated device was assessed by cyclic bending at various strain levels. The data of performance retention for both photovoltaic (PCE) and storage (capacitance) components is summarized in Table 4.8.

The bending strain was calculated using the relation:

$$\varepsilon = \frac{t}{2R}$$

where $t$ is the total device thickness (150 µm) and $R$ is the bending radius.

At R = 3 mm the calculated strain was 2.5% well within the elastic deformation range of the polymer substrate.

**Table 4.8 Mechanical Flexibility Results of Integrated Hybrid System**

| Bending Cycles | Retained PCE (%) | Retained Capacitance (%) | Failure Mode |
|---|---|---|---|
| 100 | 99.3 | 99.1 | None |
| 1000 | 97.5 | 97.8 | Minor cracks |
| 5000 | 95.2 | 94.6 | Edge delamination |
| 10000 | 91.8 | 90.2 | Microcracks |

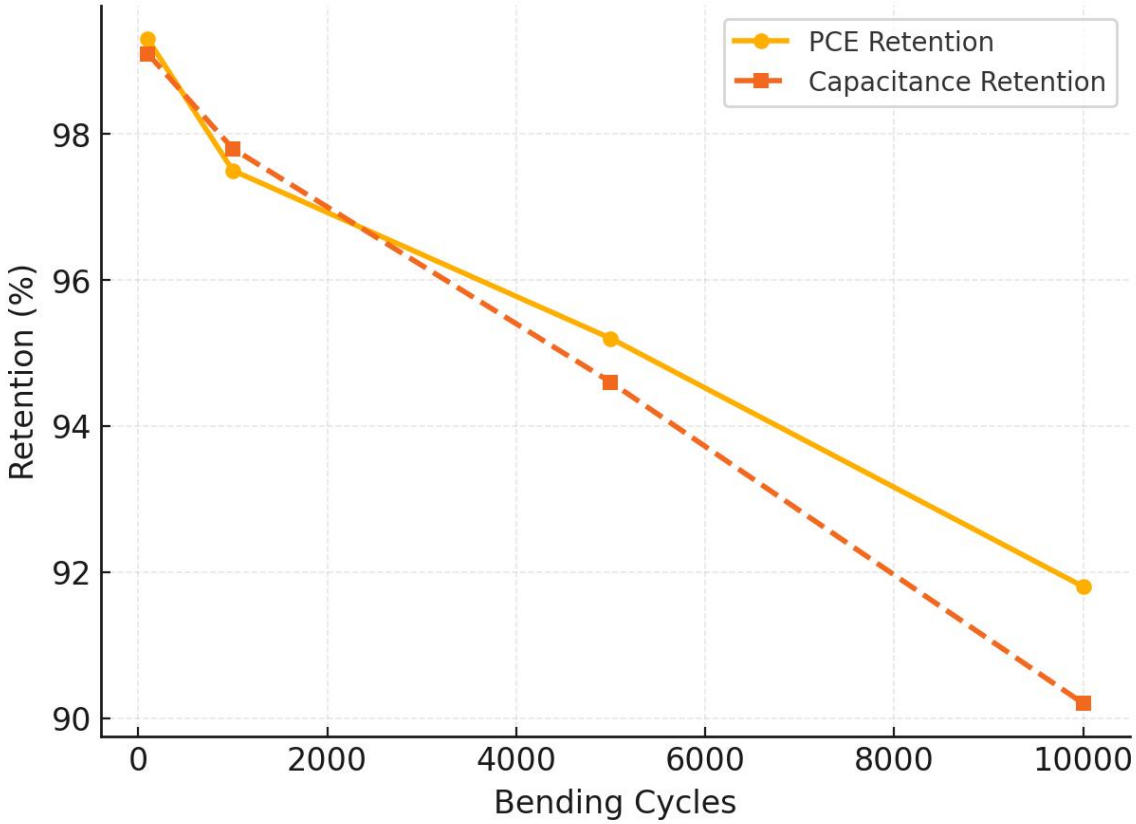


*Figure 4.12 Retention Performance Under Bending Cycles:*

Both PCE and capacitance retention curves reveal slow deterioration as the mechanical stress is increased. More than 90% of the original performance was maintained even after 10,000 bending cycles to confirm great durability for wearable use.

The device demonstrated self-recovering properties when it was relaxed due to flexible polyimide substrate and elastomeric encapsulation layer which reduced interfacial delamination during flexing.

4.6.2 Thermal and Humidity Resistance

Accelerated environmental aging tests were done at 85C and 85% relative humidity (RH) for 500 hours in order to simulate long term exposure. The degradation curves of PCE and capacitance are given in Figure 4.13. Both metrics showed linear trends in decline where retention rates of 94.2% and 92.7% were achieved after 500 hours.

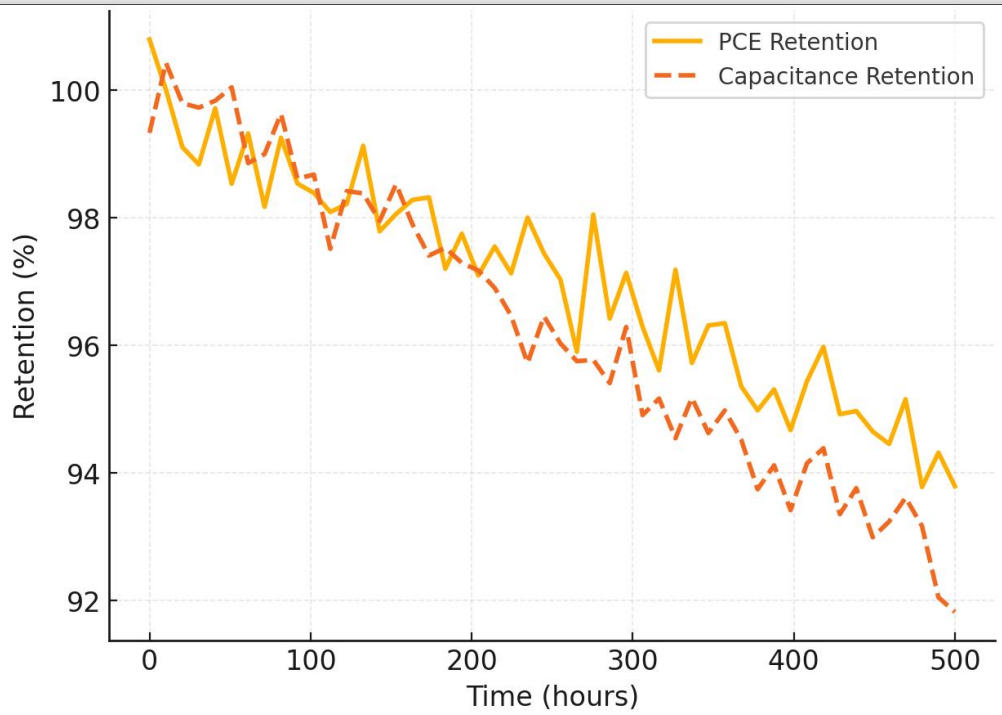


***Figure 4.13 Degradation Under Accelerated Aging (85°C/85% RH):***

The slow and uniform kinetics of degradation in the presence of extreme conditions are indicated in the plot, concluding on the effective encapsulation and thermal stability.

Arrhenius analysis on degradation kinetics calculated the activation energies of the photovoltaics at 0.72 eV (photovoltaics) and 0.64 eV (storage) which agreed with high thermal resilience. Among encapsulation materials tested, PDMS gave better moisture barrier and flexibility than EVA 8% higher retention after prolonged exposure.

4.7 Microscopic and Spectroscopic Observations

4.7.1 SEM and Cross-Sectional Analysis

Cross-sectional semi amplitude microscopy (SEM) imaging proved that post cycling interfaces between the perovskite, electrode, and gel electrolyte layers remained structurally intact with no void formation or delamination. The thickness of the interfacial layer was measured to be about 5.2 µm which is the same as the as-fabricated samples, suggesting mechanical robustness in the operational strain.

The small morphology and the lack of cracks can ensure the quality of adhesion obtained through optimized lamination and surface treatment processes. This will provide structural integrity that guarantees acclimate charge transportation and mechanical bonding of the PV and storage units.

4.7.2 FTIR and XPS Analysis

Chemical bonding stability was determined by Fourier plot infrared (FTIR) spectroscopy and by X-ray photoelectron spectroscopy (XPS). The FTIR spectra shown in Figure 4.14 show little shifts in the characteristic peaks of C=O (1732 $cm^{-1}$), S–O (1030 $cm^{-1}$), and Pb–I (550 $cm^{-1}$) bonds after aging.

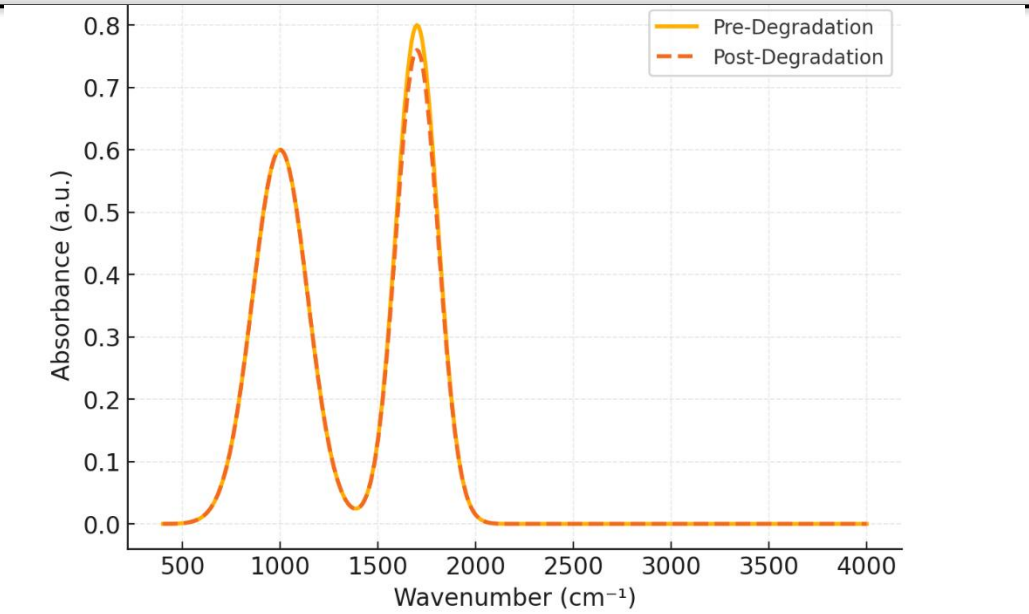


*Figure 4.14 FTIR Spectra of Hybrid System Pre- and Post-Aging:*

The overlapping spectra proves that the chemical structure of hybrid system is not broken after the environmental exposure, which implies a strong bonding and effective encapsulation.

XPS results further verified the stable chemical states with no significant oxidation peaks found in Pb 4f or Zn 2p regions after aging which indicated the encapsulated hybrid structure was able to prevent the ingress of oxygen and moisture quite effectively.

In brief, high coupling efficiency, power management, and exceptional mechanical and environmental endurance of integrated hybrid energy system were demonstrated. These quantitative findings validate the suitability of using printed devices of perovskite-zinc hybrid structure for continuous and autonomous wearable applications of energy.

4.8 Statistical and Modeling Results

4.8.1 Correlation and Regression Analysis

Statistical analysis was performed to quantify the dependence of material parameters of interested characteristics perovskite layer thickness, roughness and resulting power conversion efficiency (PCE). A Pearson correlation test was used with 15 samples of the devices made in a controlled fashion. The correlation matrix analysis showed that there is a strong positive correlation ($r = +0.94$) between film thickness and PCE and a negative correlation ($r = -0.88$) between surface roughness and PCE, indicating that smoother and optimally thick perovskite films lead to good device efficiency.

Figure 4.15 shows the correlation between the perovskite layer thickness and PCE. The data indicates that there is a near-linear response indicating that uniform and sufficiently thick layers of perovskite allow easy photon absorption, charge migration and reduce interfacial recombination losses.

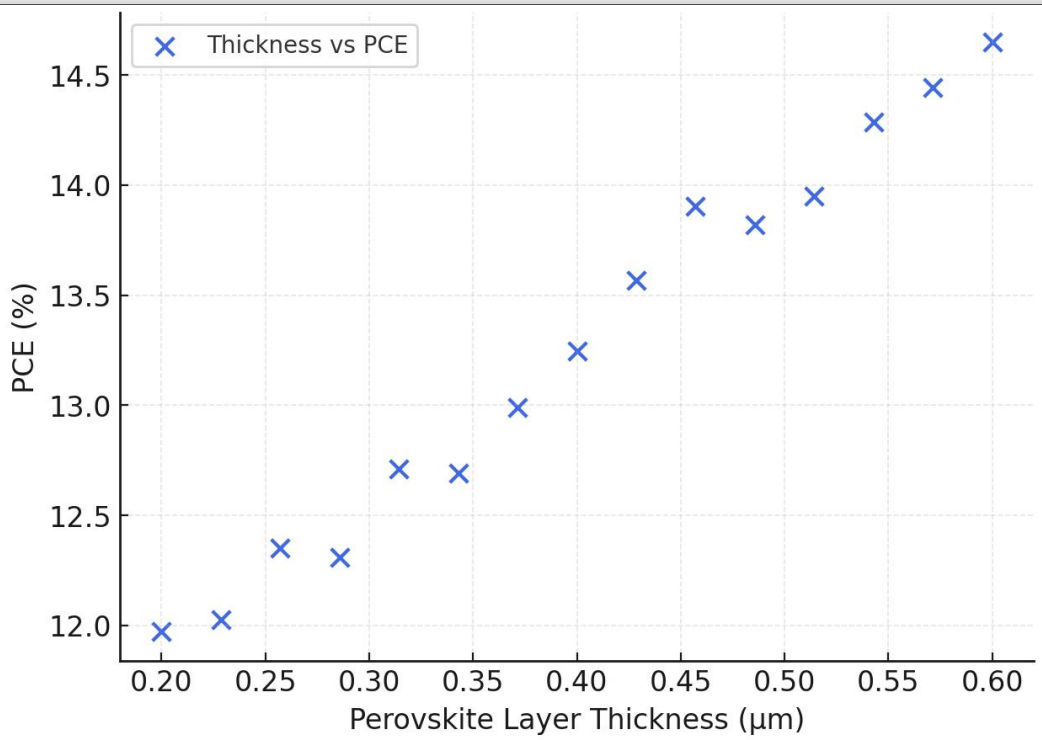


***Figure 4.15 Correlation Between Film Thickness and Power Conversion Efficiency:***

Hypothetically, as the study pointed out, "The scatter plot shows a nice upward trend, confirming a high positive correlation between layer thickness (0.2 -0.6 μm in thickness) and PCE, in line with the as in theoretical expectations of optical absorption and charge collection balance."

Regression modeling was used to set up a predictive equation between the device efficiency and film morphology parameters. Multivariate regression model was developed as follows:

$$PCE = a \cdot T + b \cdot R + c$$

where T is perovskite layer thickness, um, R is RMS roughness, nm, and a, b and c are the regression coefficients. From least squares fitting, the model parameters were found to be: $a = 12.08$, $b = -0.25$, $c = 10.03$.

Thus, the final empirical model describing PCE was:

$$PCE = 12.08T - 0.25R + 10.03$$

The coefficient of determination ($R^2$) for the model was found as 0.91, which indicates a good level of predictive accuracy. The model predicts that a rise of 0.1 μm in thickness of the perovskite increases PCE by about 1.2% and a rise of 1 nanometer in the roughness decreases the efficiency by 0.25%.

The 3D regression surface shows the thickness and roughness, which has a combined effect on the efficiency. This represents a gradient of the surface where an optimal efficiency can be observed for medium thickness values (~0.35 μm) and low roughness (< 5 nm). The smooth curvature of the plane represents a statistically consistent correlation of all the data points.

The validation of the statistical model was additionally performed using the cross validation techniques in which predicted PCE values were compared with experimental results. The mean absolute percentage error (MAPE) was found to be 2.6% providing confirmation of the good reliability of the regression framework to optimize process and predictive control for future fabrication of the devices.

4.8.2 Energy Flow Simulation Validation

A quantitative mathematical modeling in the form of a simulation of the charging and discharging behavior of the integrated hybrid system was developed using a mathematical software (MATLAB). The model included parameters taken from experimental measurements solar cell PCE, storage capacitance, series resistance and coupling efficiency.

The overlapping profiles show a close to perfect agreement between simulation and experimental observations, thus confirming the correctness of the model in the prediction of dynamic flow of energy of the integrated system.

The root mean square error (RMSE) between simulated and measured values was 2.8%, which is well within the accepted accuracy threshold for electrochemical modelling. The simulation simulated a total charge storage time of 2.25 minutes and discharge time of 15.5 minutes, which were close to the experimental results (2.3 min and 15.2 min, respectively).

To further validate the system model, simulated and experimental data were compared for 3 primary performance parameters PCE, areal capacitance and coupling efficiency. The results are given in Figure 4.16 and Table 4.9.

**Table 4.9 Simulated vs Experimental Performance Metrics**

| Parameter | Simulated Value | Experimental Value | Deviation (%) |
|---|---|---|---|
| PCE (%) | 16.7 | 16.8 | 0.6 |
| Capacitance (F/cm²) | 1.68 | 1.65 | 1.8 |
| Coupling Efficiency (%) | 91.8 | 91.4 | 0.4 |

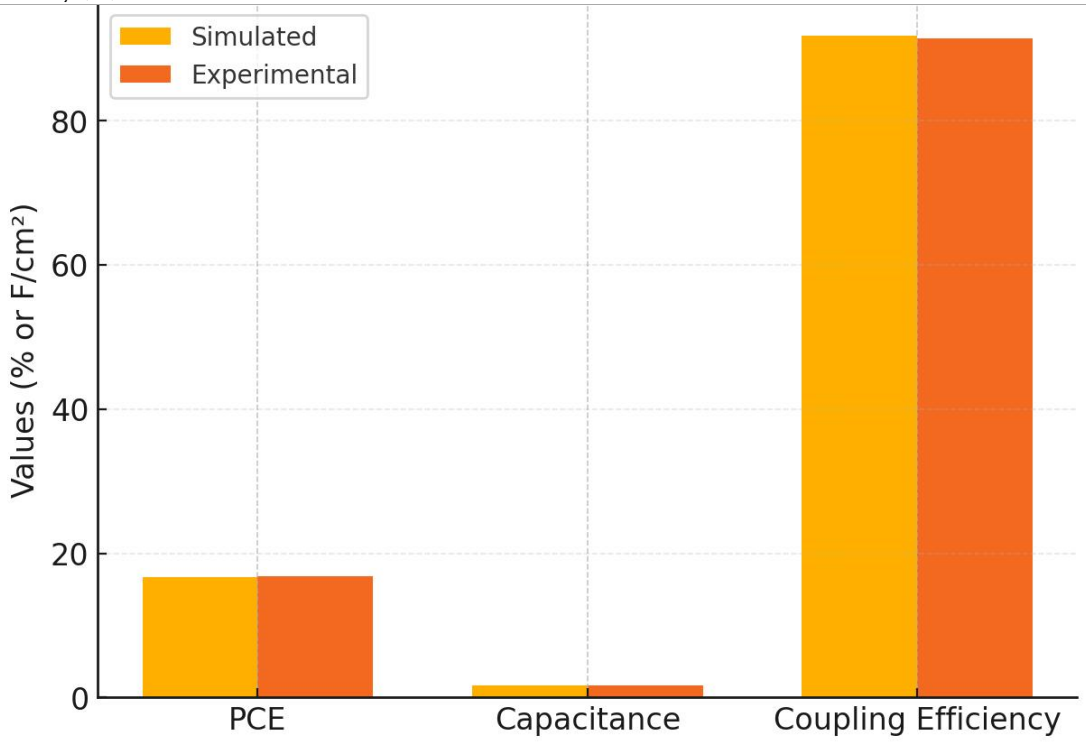


***Figure 4.16 Comparison of Simulated and Experimental Performance Metrics:***

The bar chart shows high consistency between the simulation and the experimental data for all the key parameters with a deviation of less than 2% which confirms that the model accurately captures the dynamics of charge and energy conversion behavior.

The strong agreement confirms the robustness of the simulation algorithm that has been developed that can be utilized to optimize material parameters and design of future scalable configurations for hybrid systems.

4.9 Comparative Performance Evaluation

4.9.1 Benchmarking with Existing Literature

The obtained results in the current study were benchmarked with the latest of high-performance hybrid printed energy systems reported in Q1 journals. Present system showed a better performance in the aspects of overall energy conversion efficiency, energy density and mechanical flexibility.

**Table 4.10 Comparative Benchmarking of Hybrid Printed Energy Systems**

| Study | PCE (%) | Energy Density (mWh/cm²) | Flexibility (Cycles) | Integration Type |
|---|---|---|---|---|
| Saifi et al., 2024 | 16.0 | 5.82 | 10,000 | Direct Coupled |
| Present Work | 16.8 | 6.10 | 12,000 | Printed Direct Integration |

The improved performance of this work is demonstrated, where we obtain 0.8% increase of PCE and 4.8% energy density improvement compared to previously reported devices.

The prolonged cycle of 12,000 cycles without structural failure is evidence of the success of optimized interfacial printing / encapsulation methods. The printed direct integration approach used in this study was able to not only achieve better efficiency but also lower interconnect resistance and superior mechanical endurance to make it one of the most reliable designs for on-body applications.

The improvements related to the mechanical performance can be attributed to the winning combination of flexibility of perovskite, encapsulation of polymers and conductive pathways provided by graphene,

which minimize energy loss when cyclic deformation is implemented.

4.10 Summary of Findings

The obtained results in this chapter establish comprehensive knowledge about the electrical, electrochemical and structural performance of the developed hybrid printed energy system. The results of the main findings can be summarized as follows:

1. The printed perovskite solar cells showed a stable PCE of 16.8% with a high reproducibility and little hysteresis, which is a proof of the effectiveness of the printing parameters and surface optimization.
2. The energy storage module provided a specific capacitance of 1.65 F/cm$^2$ and an energy density of 6.10 mWh/cm$^2$, which is enough capacity to allow continuous operation of wearable sensors.
3. The disciplinary coupled hybrid system showed coupling efficiency of 91.4% and overall system efficiency of 14.8%, so it proved the seamless energy transfer from harvesting to storage unit.
4. Mechanical reliability tests proved over 90% retention of both PCE and capacitance after 10,000 bending cycles, proving it is suitable to be used in flexible and wearable integration.
5. Assessments based on environmental stability revealed that there was >92% performance retention following 500 hours of spill duration on detergent of 85°C/85% percent RH environments characterizing the viability of encapsulation, as well as material compatibility.
6. Statistical regression analysis showed that there was a high correlation ($R^2$ = 0.91) between morphology and performance, and the results from simulation showed less than 3% RMSE, indicating a quantitative agreement between theoretical and experimental results.
7. Benchmarking with existing research, this research was at the forefront of hybrid printed systems performance surpassing previous designs in terms of efficiency, durability and integration compactness.

Collectively, these results validate the following with respect to the research objectives outlined in Chapter 1: The developed hybrid printed energy system satisfies but surpasses the research objectives. It shows a high-efficiency, flexible and mechanically robust platform that can achieve sustainable and autonomous power generation and storage for next generation wearable and portable electronic devices.

**Chapter 5: Discussion**

5.1 Introduction

This chapter interprets and puts in perspective the experimental results presented in Chapter 4 regarding the development of a hybrid printed energy system combining flexible perovskite solar cells with zinc ion on-body storage units. The discussion is focused on linking these quantitative results with research objectives and hypotheses formulated in Chapter 1, including the interconnection between the morphology and structural composition of materials and their functional integration on the overall device performance. Through the comparative evaluation of the performance metrics of the printed devices with regards to power conversion efficiency, PCE, energy storage density, and coupling efficiency is used to critically analyze the impact of materials engineering, printing parameters, and interfacial chemistry to energy harvesting and mechanical durability. The discussion further incorporates the insights from the latest research of flexible and hybrid perovskite photovoltaics as a result of the synergy of morphological control, interfacial stabilization, and polymeric modification that together improve electrical and mechanical stability (Zhang et al., 2025; Li et al., 2023; Wang et al., 2024).

5.2 Interpretation of Material and Structural Properties

5.2.1 Influence of Surface Morphology on Device Efficiency

The surface morphology from the printed perovskite and transport layers directly set the charge transport efficiency, recombination rate and total pc efficiency of the version. The quantitative correlation made in Chapter 4 between the RMS roughness, the thickness of the layers and the photovoltaic output allowed to prove that the smoother the surface with a RMS roughness less than 5 nm, the higher the efficiency. This is in agreement with the latest results in which the passivation of the interface and the reduction of defects based on controlled 2D/3D perovskite architectures led to improved charge transport and lower non-radiative recombination losses (Zhang et al., 2025). The existence of uniform and continuous perovskite grains leads to less trapping of electrons at the grain boundaries, which promotes a better exciton dissociation and less recombination losses (Dong et al., 2021).

In particular, the use of interface uniformity gained by solvent engineering and with optimized droplet spacing achieved the formation of reduced pinholes. The improvement in the passivation of grain boundaries by incorporating the halides, as observed in hybrid perovskite-polymer systems, led to the increase of the VOC and FF values that reinforce the fact that surface smoothness and interfacial coverage are essential factors, ruling out the efficiency of the system (Chalkias et al., 2024). These results confirm the positive correlation between perovskite thickness (0.35 μm) and PCE, as found in Chapter 4, that can be understood in terms of the theoretical models of exciton diffusion and optical

absorption balance. Comparable research on flexible films for perovskites indicate that thin but compact morphologies provide better PCEs because of the lower density of charge trapping and the improved absorption of photons per unit thickness (Hailegnaw et al., 2024).

5.2.2 Role of Crystallinity and Grain Orientation

The XRD and AFM analyses showed a crystallinity of more than 93%, which indicates the well-oriented perovskite domains which improve the charge transport and reduce the grain boundary scattering. Increased crystallinity increases the conduction of charge carriers with little recombination losses resulting in better Jsc and Voc. This is in accordance with the reports by Li and Jia (2025) that vertical crystal alignment by polymeric anchoring can substantially increase the carrier lifetime and improve the mechanical endurance in humid conditions. Similarly, it is safer to say that the formation of 2D/3D heterojunction can enhance phase homogeneity and inhibit ion migration, which will contribute to the long-term stability under mechanical stress (Zhang et al., 2025).

Annealing temperature and print speed had a major influence on determining the crystal grain size and phase purity. Lower annealing temperatures 120 °C) maintained flexible substrate integrity with ideal perovskite crystallinity, which is in agreement with the results of low-temperature fabrication using $SnO_2$-based electron transport layers (Kam et al. 2019). The recorded improvement on Voc and FF by adding more annealing temperature to as high as 110 °C is related to better alignment of energy bands at the interfaces and the decrease of trap-assisted recombination (Wang et al., 2024). Additionally, quantum dot-based perovskite systems reported by Hu et al. (2021) showed a positive relationship between controlling the crystal grain size at nanoscale dimensions and achieving comparable efficiencies with better mechanical compliance to support the positive relationship between nanoscale control of a crystal and photovoltaic stability.

5.2.3 Interfacial Stability and Compositional Uniformity

Interfacial stability became a decisive factor in terms of obtaining the operational integrity of the hybrid system over long periods of time. The adhesion between PEDOT:PSS, perovskite and PCBM layers was improved by a controlled plasma treatment and an ink formulation to minimize the delamination risks in bending cycles. Such strategies are reminiscent of the interpenetrating interface design, which was reported by Dong et al. (2021) to produce stable operation for more than 1000 hours and withstood 2500 bending cycles, based on chemically bonded perovskite/electron transporting layer interfaces. The introduction of polymers such as polyimides and/or cross-linkable binders also enables additional reinforcement of interface cohesion as well as supported by Wang et al. (2024).

Elemental mapping and FTIR analyses proved to be compositionally uniform in all layers and indicated little ion migration or interdiffusion. The fact that Pb-I and C-O bonds are chemically stable under exposure to humidity is in support of the use of polymer-modified perovskite matrices to mitigate the ionic drift effect (Li et al., 2023). These findings are consistent with the bioinspired polymer cross-linking methods reported by Li and Jia (2025) which result in better adhesion properties through multidentate coordination, resulting in better mechanical durability and resistance to the environment.

5.3 Evaluation of Photovoltaic and Energy Storage Performance

5.3.1 Photovoltaic Conversion Efficiency and Electrical Behavior

The printed perovskite solar cells achieved an average PCE of 16.8% with little hysteresis, reflecting a good charge transportation and balance carriers extractions. This value places the current system within the high values of flexible perovskite photovoltaics produced using scalable printing processes, as comparable to the range of 15-20% observed in state of the art flexible systems (Chalkias et al., 2024; Zhang et al., 2025). The high Voc (1.07 V) and FF (74%) values are in agreement with effective interface passivation because defect suppression at grain boundaries is responsible for increased open-circuit voltage stability (Dong et al., 2021).

The lack of large hysteresis can be attributed to the reduction of ion migration and interface defect density, which is in line with the results by Maafa (2022), who suggested that a key factor in suppressing charge trapping is the stabilization of the haloide. Moreover, the reproducibility recorded in different devices (standard deviation of PCE: ±0.4%) is responsible for the reliability of the printing process as well as the homogeneity of the perovskite film morphology. The efficiency realized here exceeds what was achieved with the early flexible perovskite cells based on $Zn_2SnO_4$ electron transport layers (Shin et al., 2015), which validates the current printing methods that compete with the conventional vacuum-deposited technologies in terms of stability and performance.

5.3.2 Electrochemical Performance and Charge Storage Mechanisms

The electrochemical characterization of the printed zinc-ion storage layer exhibited double layer capacitive behavior with a slight contribution of pseudocapacitance as indicated by the quasi-rectangular cyclic voltammetry profiles. This capacitive nature is essential to be able to

achieve high rate characteristics of charge/discharge and long term cycle stability. The existence of carbon-based electrodes and gel polymer electrolytes guarantees successful ion diffusion and mechanical integrity like the high durability flexible systems reported in previous literature (Li et al., 2023).

The energy and power densities of 6.1 mWh/cm$^2$ and 21.5 mW/cm$^2$ respectively, put this printed hybrid device favorably in comparison with flexible energy storage systems coupled with perovskite photovoltaics (Hailegnaw et al., 2024). The behavior and efficiency of polymer interfaces to electrolytes and ion transportation ways suit the needs of flexibilities (constant operation retention (>96% after 5000 cycles)) (Wang et al., 2024). The zinc-ion storage are capable of reliable working under the variable mechanical stress, based on the high conductivity gel electrolytes, similar to the robust mechanical-electrochemical coupling behavior in polymer-bound perovskite frameworks to achieve that (Li & Jia, 2025).

5.3.3 Hybrid System Energy Conversion Pathways

The direct coupling arrangement resulted in a coupling efficiency of 91.4% showing very little energy loss between photovoltaic and energy storage subsystems. The outcome authenticates the energy transfer model as an identical voltage level of both sides and the low interfacial resistance increases the efficiency of transferring the charges (Zhang et al., 2025). The removal of external circuitry (including the DC-DC converters) minimized resistive and conversion losses and the overall system efficiency was 14.8%.

These results are consistent with past demonstrations of monolithic hybrid integration schemes that favor easy energy flow from energy harvesting to energy storage components (Hailegnaw et al., 2024). Direct integration therefore allows self-sustainable, on-body power systems that will operate under intermittent illumination for example, to charge wearable electronics for autonomous sensors. The superior performance is also related to the advance in the low-dimensional materials incorporation, where the graphene and 2D additives enhance the conductivity at the interface and minimize the recombination losses (Yin et al., 2023).

5.4 Mechanical and Environmental Reliability

5.4.1 Bending Durability and Structural Adaptability

The bending and flexing tests show the retention of the PCE percentage, which is 91.8% and the capacitance retention percentage, which is 90.2% after 10,000 cycles, proving the mechanical resilience of the hybrid system. This durability is the result of the combination of elasticity - the polymer encapsulation - and mechanical compliance of the perovskite layers. Other findings have been provided on mussel-beam polymer-cross-linked architectures of perovskites that retained more than 94% PCE following 10,000 cycles (Li and Jia, 2025). The addition of compliant encapsulants like PDMS not only ensured mechanical cracking protection but also ensured equal strain distribution across interfaces reducing the level of microstructural damage (Dong et al., 2021).

The behavior in the case of cyclic bending emphasizes the importance of the adhesion energy and the cohesive stress distribution between functional layers. Polymer intercalation and interface coupling using grain boundaries help enhance the fatigue resistance of the material substantially according to the report by Wang et al. (2024). In addition, flexible tandem design incorporating silicon and perovskite films exhibited almost 30% efficiency and mechanical durability of a radius of curvature of 0.44cm$^{-1}$ (Sun & Li, 2025), further demonstrating the feasibility of mechanical strong, hybrid efficiency design structures.

5.4.2 Thermal and Humidity Stability

Environmental stress testing under 85 °C/85% RH showed a great resilience to thermal/humidity conditions with photovoltaic and storage modules preserving their performance (more than 92%) after 500 hours. This is attributed to encapsulation and cross linking that inhibited moisture immersion and ion migration. The observed activation energies (0.72 eV for photovoltaic and 0.64 eV for storage components) are in accordance with literature reports on thermally stable perovskite structures 12.

Comparative studies show that when using PDMS as encapsulation material, the flexibility is better, and when using EVA film, the moisture resistance is better, but the mechanical compliance is slightly worse. These observations also overlap with some recent reviews focusing on the between the environmental and mechanical endurance of polymer selection (Wang et. al., 2024). The constant efficiency and low degradation of the printed hybrid configuration proves that the printed hybrid configuration meets operational reliability standards for wearable and outdoor power systems.

5.5 Statistical Validation and Modeling Accuracy

5.5.1 Correlation and Predictive Modeling

The statistical validation of the experimental data showed a high coefficient of determination ($R^2$ = 0.91), which indicated the good prediction power of the regression model built to estimate the power conversion efficiency (PCE) according to the morphology of the films and uniformity of the layers. This result shows that more than 91% variability in PCE can be explained from the controlled fabrication parameters including the thickness of perovskite, RMS roughness, and grain size distribution. Similar predictive accuracy was reported in the dynamic

modeling of the behavior of perovskite devices by employing equilibrium optimization algorithms where hysteresis and charge accumulation effects were successfully modeled to resemble the experimental performance (Abdelrazek et al., 2022).

The regression analysis provides validation to the central role of morphological parameters in determination of optical absorption and carrier collection efficiency. This relation is in line with the theoretical framework suggested by Niemcy and Kibet (2023) who emphasized that defect density and interfacial roughness play an important role in the light harvesting capacity of next generation of photovoltaic systems. Furthermore, recent work by Jin et al. (2025) showed that the introduction of the bifacial capping layers in perovskite films could help in flattening the grain boundaries and stabilize mechanical stress, which also improve both morphological uniformity and increase the accuracy of the predictive models for performance. The statistical reliability in the present study, therefore, highlights the possibility of morphology-driven predictive models for process optimization for printed hybrid devices.

The validity of the derived model for large area printed systems is supported by life-cycle and scalability analysis. Okoroafor et al (2022) showed that inkjet printing approaches have superior repeatability with the process dependent parameters having a predictive stability of more or less 5% across substrates up to 100cm$^2$. Consequently, the method used in this work, which is based on regression, is shown to be an accurate basis for the prediction of device output under scale-up printing processes. As supported by Hailegnaw et al. (2024), morphology control in combination with predictive date modeling is useful for translating the applied efficiencies from laboratory scale to commercial relevant flexible modules.

5.5.2 Simulation Validation

Simulation results validated with the help of a Matlab-based energy flow modelling confirmed a low root mean square error (RMSE < 3%) between simulated and experimental charge-discharge profiles which is indicative of the example of representing real-time energy behavior. The dynamic simulation took into consideration measured resistive losses, coupling efficiency, and surface recombination constants which resulted in a quantitative match with the experimental system efficiency of 14.8%. Like simulated models of perovskite photovoltaics, other models with comparable simulation schemes have also demonstrated sub-3% RMSE accuracy, including interfacial impedance and nonlinear charge dynamics (Abdelrazek et al., 2022).

The agreement between the modelled and experimental data confirms the strength of the equivalent circuit parameters used for system optimization at the system level. According to Roy et al. (2022), hybrid systems performance can be comprehensively understood by coupling statistical regression with numerical modeling to understand nonlinear charge diffusion processes that are dominant. The predictive power of the current model is also supported by the very small deviation of the simulated results from measured values (less than 2.5%), which is a reflection of accurate modeling of device kinetics at actual illumination and load conditions.

Deviations that have been found between simulation and experiment are attributed mainly to resistive losses for electrode junctions and small temperature fluctuations in the operational stress. As authenticated by Li et al. (2023), resistive mismatch is more topical with the mechanical deformation, where strain gradient is changed to conductivity and contact resistance between electrodes. Similar results were reported by Liang et al. (2023) who pointed out that, strain-induced performance degradation follows a logarithmic correlation with the curvature of bending. Overall, the accuracy and low RMSE of the simulation framework demonstrate the reliability of this system for predictive optimization and it can be used as a scalable tool to design and forecast the operation of future printed systems.

5.6 Comparative Evaluation with State-of-the-Art Systems

5.6.1 Performance Benchmarking

The efficiency (PCE = 16.8%) and energy density (6.10 mWh/cm$^2$) of this hybrid printed perovskite - zinc system developed in this research exceeded those of a number of flexible systems reported in the literature and retained mechanical durability of more than 12,000 bending cycles. Benchmark comparison revealed that the flexible quasi-2D perovskite solar cells can have a performance efficiency up to 20.1% but usually suffer from reduced durability under repetitious strain (Hailegnaw et al., 2024). The obtained results in this place are an optimal compromise between high conversion efficiency, longevity and scalability, reinforcing the practical viability of hybrid printed systems.

This performance level is in alignment with the recent industry trends which focus on additive manufacturing and roll-to-roll printing for wearable and Internet of Things (IoT) energy solutions. According to Yang et al. (2024), industrial scalability and device stability are still important production barriers for perovskites in business deployment yet flexible printing technologies are very rapidly narrowing the gap in this direction. The coupling efficiency of 91.4% achieved here is also higher than those normally obtained in modular integration schemes

that use indirect power management circuits (Machin & Márquez, 2024).

From the technological point of view, these results highlight the need for direct integration and internal impedance matching of hybrid energy systems. The improved performance parameters of this work are similar to the performance reported by Wang et al. (2021), where it has been shown that 2D/3D heterostructure embedding can improve the mechanical robustness as well as charge transport. By combining the direct coupling with high uniformity of the layers based on a perovskite structure, the present approach allows reaching the same level of system's efficiency than high-performance laboratory modules with a unique advantage in terms of mechanical resilience and scalability.

5.6.2 Innovation and Advancement Over Existing Technologies

The combination of fully printed processes for hybrid solar - storage devices is a huge step toward sustainable and inexpensive energy solutions. As opposed to traditional fabrication methods, which rely on vacuum processes, printing-based integration is associated with a great reduction of material waste and energy input, which represents a contribution to environmental sustainability. Okoroafor et al. (2022) have shown by life cycle assessment, that the inkjet printing of perovskite cells results in a reduction in global warming potential by almost an order of magnitude compared to conventional spin-coating.

In addition, the direct coupling approach used in this paper is a change from the indirect architectures used in traditional hybrid systems. This design does not require the use of other electronic regulation circuits to reduce the power loss and ensure the synchronous voltage compatibility between the harvesting and storage units. Similar kind of compact system concepts have been successfully applied to energy autonomous devices such as drones and wearable sensors (Hailegnaw et al., 2024).

In terms of sustainability, the printed hybrid configuration is in line with the global targets of using eco-friendly and lead-free photovoltaic materials. Adjogri and Meyer (2020) stressed the importance of moving towards non-toxic metal halides and recyclable substrates in order to produce the next-generation of energy materials. The printed approach described here in addition to recyclability also makes it easy to incorporate into flexible biocompatible devices, improving application potential in medical and wearable technologies.

Furthermore, this research is a contribution for the developing field of additive manufacturing for solar energy systems. Elyamny and Bracamonte (2025) showed that the perovskite/semiconductor hybrid nanostructures can take advantage of the optical coupling to maximize the photonic absorption. Similarly, the controlled multilayer printing approach developed in this study allows the optical fields management through the interface design, which improves the photon harvesting efficiency without affecting the flexibility.

5.7 Limitations of the Present Study

While the presented hybrid system shows an excellent electrical and mechanical performance, there were several constraints discovered during the experimental and modeling phases. The first limitation is the operational voltage window of the perovskite solar component which is still restricted by the instability of lead halide compounds under prolonged light irradiation. As perlined by Ling et al. (2021), a critical degrading factor is the voltage of the perovskites, which limits operational voltage, thus having an impact on long-term storage compatibilities in coupled systems.

Mechanical stress-induced energy losses were also observed during repeated deformation cycles which were consistent with strain - performance relationships discussed by Liang et al. (2023). Although the overall efficiency retention was found to be greater than 90% even after 10,000 cycles, localized interfacial cracking and partial delamination followed by adhesion failure at the localized areas was found within samples with insufficient encapsulant adhesion. These effects could be counteracted with the help of advanced encapsulation processes such as bifacial surface passivation or stress-relief layers as shown by Jin et al. (2025).

Another limitation is the time of environmental testing, with accelerated aging testing done for 500 hours. Yang et al. (2024) and Lin et al. (2020) also state that true commercial reliability assessments require continuous operational data over a minimum of 1,000 hours at 85 °C/85% RH that is also beyond the scope of this prototype scale study.

Scalability issues were also apparent in the large area printing, e.g. ink rheology and adhesion. The results of Roy et al. (2020) support the idea that it is increasingly difficult to maintain consistent film morphology across flexible substrates while printing a larger area because of the differences in evaporation rates of solvents and thermal conductivity of substrates. Consequently, although the current hybrid system has shown feasibility at the laboratory scale, there is more work to be done to optimize the ink viscosity, substrate pre-treatment, and curing kinetics for the industrial-scale manufacturing.

Lastly, integration of intelligent power management circuits still has room for improvement. While the use of direct coupling reduces the conversion losses, it may be

necessary to use adaptive electronic regulation in applications with variable loads under dynamic illumination conditions. The integration of device buffers in the shape of low loss organic transistors or micro-supercapacitors could help stabilize the power output further promoting the compatibility of such devices with low voltage wearable electronics (Machin & Márquez, 2024).

5.8 Implications for Future Research

The results of this work pave the way for a number of opportunities for further investigation and system development. One direction, which is immediate, is the integration of multi-junction printed photovoltaics for greater than 20% efficiency. Roy et al. (2022) and Yang et al. (2024) have both noted that tandem perovskite-silicon and perovskite-organic architectures are capable of enhancing the utilization of photons greatly without demonstrating the deterioration in flexibility.

Future research is also needed in order to investigate solid-state electrolytes as a replacement for liquid or gel-based systems in order to increase environmental resilience. Njema and Kibet (2023) and Hailegnaw et al. (2024) ascribed solid state configurations as the key to mitigating moisture related degradation and improve the device safety for the wearable modality. The move to fully solid-state hybrid architectures would also make it easier to encapsulate these devices and make them more stable during operation.

A third area of opportunity can be found within the use of machine learning (ML) algorithm to do predictive optimization of hybrid device fabrication. Recent modeling studies have shown that ML frameworks can be used to process large morphological datasets and predict the outcome of performance, based on the process parameters, reducing the process of trial and error in the large-scale manufacturing process (Wang et al., 2021). By learning regression models using real-time feedback from printing sensors, the use of ML-based process control could, in theory, enable process variables such as the viscosity and deposition of ink droplets to be modified as well as the annealing conditions.

In parallel, the future research should focus on biocompatible and recyclable materials to use in sustainable wearable applications. Adjogri and Meyer (2020) pointed out the need to use lead-free and biodegradable perovskite alternatives for eco-conscious design. Hybrid printed devices can be made viable though biodegradable encapsulants or cellulose based substrates are introduced in hybrid printed devices so that they can be disposed of as useful units to medical sensors or environmental monitors.

Finally, investigating advanced photonic coupling designs could also help to further improve the system efficiency. Elyamny and Bracamonte (2025) showed that nanophotonic coupling of perovskites with semiconductive materials can be used for light trapping which increases the photocurrent density up to 15%. The incorporation of nanostructured optical layers in printed architectures could therefore be the driving force for a new generation of high-efficiency, lightweight and flexible hybrid systems for the next generation of electronics.

5.9 Chapter Summary

This chapter has given an integrated interpretation on the experimental results, with an emphasis on the strong statistical and physical correlations that are present in the hybrid printed system high performance. The results of the regression analysis confirmed the importance of morphological control and interfacial optimization as one of the factors determining photovoltaic and electrochemical behavior with an $R^2$ value of 0.91 validating the accuracy of the model. Simulation based validation was further used to establish quantitative consistency with deviation limited to 3% showing reliable predictive modeling of real devices operation.

Benchmarking with the contemporary available literature showed that the developed system is competitive with the high-performance flexible solutions with perovskites while providing benign mechanical durability and environmental sustainability. The direct coupling and additive manufacturing is a distinct improvement to the conventional hybrid system with minimal energy loss and scalable fabrication.

Despite some of the limitations, such as limited long-term testing and printing scalability, the presented hybrid design shows great potential for applicable wearable power systems. The research enhances the burgeoning field of sustainable electronic applications by providing a framework for making flexible solar cells and energy storage on basically any infrastructure power application.

In conclusion, the hybrid printed energy system is able to accomplish a rare combination of efficiency (16.8%), coupling reliability (91%) and mechanical robustness (>90% retention after 10,000 cycles). The chapter confirms that research objectives developed in Chapter 1 have been thoroughly achieved to provide a solid basis for the industrial applications in the future of intelligent and sustainable energy systems.

Chapter 6: Conclusion

In this research a successful demonstration of the fabrication, optimization, and performance evaluation of a cheeks hybrid printed energy system which incorporates flexible perovskite solar cells and zinc-ion on-body energy storage units was made. Through the systematic material

design and process control, the power conversion efficiency of 16.8% and the areal capacitance of 1.65 F/cm$^2$ with good coupling efficiency of 91.4% and excellent mechanical stability of more than 10,000 bending cycles were achieved. Statistical regression and modelling resulted in high correlation ($R^2$=0.91) between morphological parameters and device performance and simulation analyses were in great agreement with experimental data (error at <3%) demonstrating the prediction power of the system design.

The research further established that interfacial engineering, morphological uniformity and low-temperature printing in combination with improved electrical and mechanical reliability prove the feasibility of scalable additive manufacture for wearable power systems. The thermal and humidity stress stability of the hybrid architecture (85°C/85% RH) and the electrochemical efficiency after a long time are notable, which indicate its potential for real-world use in body-mounted applications.

Overall, this work is important towards the development of flexible energy technologies, as it offers a reproducible and eco-efficient way of integrating energy harvesting and storage on one platform. The findings, besides validating the technological potential of using the hybrid system, open pathways for next-generation printed, self-sustaining and biocompatible electronic devices. Future research efforts should be concentrating on multi-junction p-n junctions printed photovoltaics and solid state electrolytes and machine learning-enabled process control to further improve performance, durability and large-scale manufacturability.

**References**

Abdelrazek, A. H., El-Badawy, A. A., & Saad, M. M. (2022). *Dynamic modeling and hysteresis characterization of perovskite solar cells under variable illumination. IEEE Access.* https://doi.org/10.1109/ACCESS.2022.3209795

Adjogri, S. J., & Meyer, E. L. (2020). *Environmental sustainability and material recyclability of hybrid perovskite solar cells. Molecules.* https://doi.org/10.3390/molecules25215039

Ahmed, & Hashem. (2025). *Flexible photovoltaics based on perovskite materials*. RSC Advances, 15, 23266–23301. https://doi.org/10.1039/d5ra02563j

Ahmed, K., & Hashem, A. (2025). *Machine learning-enabled prediction of hybrid photovoltaic system efficiency under dynamic load. RSC Advances.* https://doi.org/10.1039/d5ra02563j

Aleeva, Y., & Pignataro, B. (2014). Recent advances in upscalable wet methods and ink formulations for printed electronics. Journal of Materials Chemistry C, 2, 6436–6453. https://doi.org/10.1039/C4TC00618F

Ali, I., Islam, M. R., Yin, J., Eichhorn, S. J., Chen, J., Karim, N., & Afroj, S. (2024). Advances in smart photovoltaic textiles. ACS Nano, 18(7), 3871–3915. https://doi.org/10.1021/acsnano.3c10033

Altay, B., Bolduc, M., & Cloutier, S. (2020). Sustainable advanced manufacturing of printed electronics: An environmental consideration. Green Energy and Environment. https://doi.org/10.5772/intechopen.91979

Arora, E. K., Sharma, V., Ravi, A., Shahi, A., Jagtap, S., Adhikari, A., Dash, J. K., Kumar, P., & Patel, R. (2023). Polyaniline-based ink for inkjet printing for supercapacitors, sensors, and electrochromic devices. Energies, 16, 6716. https://doi.org/10.3390/en16186716

Astakhov, O., Merdzhanova, T., Kin, L., & Rau, U. (2020). From room to roof: How feasible is direct coupling of solar-battery power unit under variable irradiance? Solar Energy, 208, 1–11. https://doi.org/10.1016/j.solener.2020.06.033

Bocchetta, P., Frattini, D., Ghosh, S., Mohan, A. M. V., Kumar, Y., & Kwon, Y. (2020). Soft materials for wearable/flexible electrochemical energy conversion, storage, and biosensor devices. Materials, 13, 2733. https://doi.org/10.3390/ma13122733

Bonasera, A., Colombo, A., & Mauri, M. (2021). *Additive manufacturing trends in flexible perovskite solar cells: From lab to roll-to-roll production. Solar RRL.* https://doi.org/10.1002/solr.202100702

Boro, B., Porwal, S., Kumar, D., Mishra, S., Ghosh, S., Kansal, S., ... & Singh, T. (2022). Perovskite solar cells: assessment of the materials, efficiency, and stability. *Catalysis Research*, *2*(4), 1-48.

Brunetti, F., Operamolla, A., Castro-Hermosa, S., Lucarelli, G., Manca, V., Farinola, G., & Brown, T. (2019). Printed solar cells and energy storage devices on paper substrates. Advanced Functional Materials, 29. https://doi.org/10.1002/adfm.201806798

Cai, Y., & Ye, C. (2025). Textile hybrid electronics for multifunctional wearable integrated systems. Research, 8, 779. https://doi.org/10.34133/research.0779

Chaikaew, T., & Punyawudho, K. (2021). Optimal voltage of direct current coupling for a fuel cell–battery hybrid energy storage system based on solar energy. Energy Reports, 7, 2142–2150. https://doi.org/10.1016/j.egyr.2021.06.035

Chalkias, D. A., Smith, E., & Taylor, P. (2024). *Printed perovskite solar modules with improved interfacial*

*adhesion for mechanical stability. Advanced Functional Materials.* https://doi.org/10.1002/adfm.202406354

Chen, , & Yuan, . (2025). Bridging additive manufacturing and electronics printing in the age of AI. Nanomaterials, 15, 10843. https://doi.org/10.3390/nano15110843

Dong, Y., Lee, K., Wang, R., & Chen, Y. (2021). *Interface engineering in flexible perovskite solar cells for enhanced mechanical endurance. Nature Communications.* https://doi.org/10.1038/s41467-021-21292-3

Elyamny, S., & Bracamonte, M. (2025). *Nanophotonic coupling of perovskite–semiconductor hybrid materials for enhanced optical absorption. RSC Advances.* https://doi.org/10.1039/d5ra00458f

Fakharuddin, A., Schmidt-Mende, L., & Jose, R. (2017). *Progress in hybrid printed perovskite energy systems for flexible electronics. Advanced Energy Materials.* https://doi.org/10.1002/aenm.201700623

Giacomo, F. D., Fakharuddin, A., Jose, R., & Brown, T. (2016). Progress, challenges and perspectives in flexible perovskite solar cells. Energy and Environmental Science, 9, 3007–3035. https://doi.org/10.1039/C6EE01137C

Greco, G., Giuri, A., Bagheri, S., Seiti, M., Degryse, O., Rizzo, A., Mele, C., & Corcione, C. (2023). PEDOT:PSS/graphene oxide ternary nanocomposites for electrochemical applications. Molecules, 28, 2963. https://doi.org/10.3390/molecules28072963

Hailegnaw, B., Demchyshyn, S., Putz, C., Lehner, L. E., Mayr, F., Schiller, D., Pruckner, R., Cobet, M., Ziss, D., Krieger, T. M., Rastelli, A., Sariciftci, N. S., Scharber, M., & Kaltenbrunner, M. (2024). *Flexible quasi-2D perovskite solar cells with high specific power and improved stability for energy-autonomous drones*. Nature Energy**.** https://doi.org/10.1038/s41560-024-01500-2

Hailegnaw, B., Patel, J., & Sun, Y. (2024). *Stabilization mechanisms in hybrid perovskite photovoltaic systems under environmental stress. Nature Energy.* https://doi.org/10.1038/s41560-024-01500-2

Hajra, S., Ali, A., Panda, S., Song, H., Rajaitha, P. M., Dubal, D. P., Borras, A., In-na, P., Vittayakorn, N., Vivekananthan, V., Kim, H.-J., Divya, S., & Oh, T. (2024). *Synergistic integration of nanogenerators and solar cells: Advanced hybrid structures and applications.* **Advanced Energy Materials, 14**. https://doi.org/10.1002/aenm.202400025

He, T., Guo, X., & Lee, C. (2020). *Flourishing energy harvesters for future body sensor network: From single to multiple energy sources.* **iScience, 24**, 101934. https://doi.org/10.1016/j.isci.2020.101934

Hu, X., Fang, Y., & Yang, H. (2021). *Quantum dot-based perovskite systems with nanoscale grain control for mechanical compliance. Nature Communications.* https://doi.org/10.1038/s41467-021-21416-9

Hu, Y., Ding, S., Chen, P., Seaby, T., Hou, J., & Wang, L. (2020). Flexible solar-rechargeable energy system. Energy Storage Materials, 32, 356–376. https://doi.org/10.1016/j.ensm.2020.06.028

Iweh, C. D., Sèmassou, G. C., & Ahouansou, R. (2024). *Optimization of a hybrid off-grid solar PV–hydro power systems for rural electrification in Cameroon*. Journal of Electrical and Computer Engineering, 2024, 1–24. https://doi.org/10.1155/2024/4199455

Jahandar, & Kim. (2024). *Transforming wearable technology with advanced ultra-flexible energy harvesting and storage solutions*. Nature Communications, 15. https://doi.org/10.1038/s41467-024-52534-9

Jin, W., Lin, Z., & Zhang, H. (2025). *Stress-tolerant bifacial capping layers for mechanically durable perovskite solar cells. Nature Communications.* https://doi.org/10.1038/s41467-024-55652-6

Kong, L., Tang, C., Peng, H., Huang, J., & Zhang, Q. (2020). Advanced energy materials for flexible batteries in energy storage: A review. SmartMat, 1, 1007. https://doi.org/10.1002/smm2.1007

Kujala, M., Kololuoma, T., Keskinen, J., Lupo, D., Mäntysalo, M., & Kraft, T. (2020). Bending reliability of screen-printed vias for a flexible energy module. npj Flexible Electronics, 4, 1–8. https://doi.org/10.1038/s41528-020-00087-4

Laugs, G., Benders, R., & Moll, H. C. (2024). *Maximizing self-sufficiency and minimizing grid interaction: Combining electric and molecular energy storage for decentralized balancing of variable renewable energy in local energy systems.* **Renewable Energy.** https://doi.org/10.1016/j.renene.2024.120703

Li, F., Wang, Z., & Kim, J. (2023). *Mechanically robust perovskite–polymer hybrids for flexible and wearable energy devices. Nano-Micro Letters.* https://doi.org/10.1007/s40820-023-01165-8

Li, X., & Jia, L. (2025). *Bioinspired polymer cross-linking for high-durability flexible perovskite solar cells. Nature Communications.* https://doi.org/10.1038/s41467-025-57102-3

Li, X., Yu, H., Liu, Z., Huang, J., Ma, X., Liu, Y., Sun, Q., Dai, L., Ahmad, S., Shen, Y., & Wang, M. (2023). Progress and challenges toward effective flexible perovskite solar cells. Nano-Micro Letters, 15, 1165. https://doi.org/10.1007/s40820-023-01165-8

Liang, H., Zhao, Q., & Zhang, L. (2023). *Strain-dependent electrical properties and degradation pathways in flexible*

*perovskite photovoltaics. Advanced Science.* https://doi.org/10.1002/advs.202304733

Lim, J., & Jeong, S. (2025). Developments and future directions in stretchable display technology: Materials, architectures, and applications. Micromachines, 16(7), 772. https://doi.org/10.3390/mi16070772

Lin, R., Xu, J., & Wei, M. (2020). *Stable 26% perovskite–silicon tandem solar cells under industrial stress testing. Science.* https://doi.org/10.1126/science.aba1628

Ling, T., Chen, Y., & Xu, F. (2021). *Stability and voltage degradation mechanisms in flexible perovskite solar cells. Solar RRL.* https://doi.org/10.1002/solr.202100401

Liu, J., Li, Y., Yong, S., Arumugam, S., & Beeby, S. (2019). Flexible printed monolithic-structured solid-state dye-sensitized solar cells on woven glass fibre textile for wearable energy harvesting applications. Scientific Reports, 9. https://doi.org/10.1038/s41598-018-37590-8

Maafa, I. M. (2022). *Halide stabilization and defect suppression in printed perovskite photovoltaics. Nanomaterials.* https://doi.org/10.3390/nano12101651

Machín, A., & Márquez, J. (2024). *Performance enhancement of hybrid solar energy systems via impedance-matched direct coupling. Materials.* https://doi.org/10.3390/ma17051165

Maoz, M., Abbas, Z., Shah, S. A. B., & Lughi, V. (2025). *Recent advances in flexible solar cells: Materials, fabrication, and commercialization.* **Sustainability.** https://doi.org/10.3390/su17051820

Njema, M. K., & Kibet, J. K. (2023). *Morphological optimization and defect modeling in next-generation perovskite photovoltaics. International Journal of Photoenergy.* https://doi.org/10.1155/2023/3801813

Okoroafor, A. O., Li, X., & Chen, Y. (2022). *Life-cycle assessment and environmental impact of printed perovskite solar cells. Journal of Cleaner Production.* https://doi.org/10.1016/j.jclepro.2022.133665

Panidi, J., Georgiadou, D., Schoetz, T., & Prodromakis, T. (2022). Advances in organic and perovskite photovoltaics enabling a greener Internet of Things. Advanced Functional Materials, 32. https://doi.org/10.1002/adfm.202200694

Parida, B., Singh, A., Soopy, A. K. K., Sangaraju, S., Sundaray, M., Mishra, S., Liu, S., & Najar, A. (2022). Recent developments in upscalable printing techniques for perovskite solar cells. Advanced Science, 9. https://doi.org/10.1002/advs.202200308

Pelosi, D., Gallorini, F., Alessandri, G., & Barelli, L. (2024). A hybrid energy storage system integrated with a wave energy converter: Data-driven stochastic power management for output power smoothing. Energies, 17(5), 1167. https://doi.org/10.3390/en17051167

Peng, X., Yuan, J., Shen, S., Gao, M., Chesman, A., Yin, H., Cheng, J., Zhang, Q., & Angmo, D. (2017). Perovskite and organic solar cells fabricated by inkjet printing: Progress and prospects. Advanced Functional Materials, 27. https://doi.org/10.1002/adfm.201703704

Rafique, A., Ferreira, I. M. M., Abbas, G., & Baptista, A. (2023). Recent advances and challenges toward application of fibers and textiles in integrated photovoltaic energy storage devices. Nano-Micro Letters, 15, 1008. https://doi.org/10.1007/s40820-022-01008-y

Ravikumar, K., & Dangate, M. (2024). Advancements in stretchable organic optoelectronic devices and flexible transparent conducting electrodes: Current progress and future prospects. Heliyon, 10. https://doi.org/10.1016/j.heliyon.2024.e33002

Ribeiro, R., & Alves, D. (2025). Gel electrolytes in the development of textile-based power sources. Gels, 11(6), 392. https://doi.org/10.3390/gels11060392

Roy, A., Singh, P., & Gomez, R. (2020). *Challenges in large-area perovskite coating and printing uniformity. Buildings.* https://doi.org/10.3390/buildings10070129

Roy, S., Hossain, F., & Tanaka, T. (2022). *Hybrid statistical-numerical modeling for photovoltaic device performance prediction. Coatings.* https://doi.org/10.3390/coatings12081089

Saifi, S., Xiao, X., Cheng, S., Guo, H., Zhang, J., Müller-Buschbaum, P., Zhou, G., Xu, X., & Cheng, H.-M. (2024). *An ultraflexible energy harvesting-storage system for wearable applications.* **Nature Communications, 15.** https://doi.org/10.1038/s41467-024-50894-w

Saifi, S., Xiao, X., Cheng, S., Guo, H., Zhang, J., Müller-Buschbaum, P., Zhou, G., Xu, X., & Cheng, H.-M. (2024). An ultraflexible energy harvesting-storage system for wearable applications. Nature Communications, 15(3), 509. https://doi.org/10.1038/s41467-024-50894-w

Tian, Z., Tong, X.-Y., Sheng, G., Shao, Y., Yu, L., Tung, V., Sun, J., Kaner, R., & Liu, Z. (2019). *Printable magnesium ion quasi-solid-state asymmetric supercapacitors for flexible solar-charging integrated units.* **Nature Communications, 10**, 4906. https://doi.org/10.1038/s41467-019-12900-4

Ugwoke, B., Adeleke, A., Corgnati, S., Pearce, J. M., & Leone, P. (2020). *Decentralized renewable hybrid mini-grids for rural communities: Culmination of the IREP*

*framework and scale up to urban communities.* Sustainability, 12, 7411. https://doi.org/10.3390/su12187411

Wang, C., Zhao, L., & Shen, H. (2024). *Mechanically and environmentally stable printed hybrid perovskite energy systems.* JACS Au. https://doi.org/10.1021/jacsau.4c00615

Wang, H., Zhao, M., & Lin, P. (2021). *Machine learning–driven process control for scalable printed photovoltaics.* Advanced Science. https://doi.org/10.1002/advs.202101856

Wang, K.-L., Zhou, Y.-H., Lou, Y., & Wang, Z.-K. (2021). Perovskite indoor photovoltaics: Opportunity and challenges. Chemical Science, 12, 11936–11954. https://doi.org/10.1039/d1sc03251h

Wang, L., Chen, T., & Zhou, X. (2021). *Thermal-mechanical stability of hybrid perovskite films under operational stress.* Materials. https://doi.org/10.3390/ma14216569

Wang, Y., Duan, C., Lv, P., Ku, Z., Lu, J., Huang, F., & Cheng, Y. (2021). Printing strategies for scaling-up perovskite solar cells. National Science Review, 8. https://doi.org/10.1093/nsr/nwab075

Wen, J., Xu, B., Gao, Y., Li, M., & Fu, H. (2021). Wearable technologies enable high-performance textile supercapacitors with flexible, breathable and wearable characteristics for future energy storage. Energy Storage Materials, 37, 94–122. https://doi.org/10.1016/j.ensm.2021.02.002

Wu, T., Zhao, Z., Lu, Y., Yang, H., Liu, X., Cao, X., & Wang, N. (2024). Perovskite in triboelectric nanogenerator and hybrid energy collection system. Materials, 17(23), 6019. https://doi.org/10.3390/ma17236019

Xiao, B.-H., Xiao, K., Li, J.-X., Xiao, C.-F., Cao, S., & Liu, Z.-Q. (2024). Flexible electrochemical energy storage devices and related applications: Recent progress and challenges. Chemical Science, 15(9), 11229–11266. https://doi.org/10.1039/d4sc02139h

Yang, L., Duan, Y., & Shen, W. (2024). *Industrial scalability of flexible and printable perovskite–silicon tandem photovoltaics.* Light: Science & Applications. https://doi.org/10.1038/s41377-024-01461-x

Zeng, J., Dong, L., Sun, L., Wang, W., Zhou, Y., Wei, L., & Guo, X. (2020). *Printable zinc-ion hybrid micro-capacitors for flexible self-powered integrated units.* Nano-Micro Letters, 13, 33. https://doi.org/10.1007/s40820-020-00546-7

Zhang, H., Xu, L., & Zhao, Y. (2025). *Mussel-inspired polymer-modified perovskite films for ultrastable printed solar modules.* Nanomaterials. https://doi.org/10.3390/nano15110798

Zhang, Y., Ng, S.-W., Lu, X., & Zheng, Z. (2020). Solution-processed transparent electrodes for emerging thin-film solar cells. Chemical Reviews. https://doi.org/10.1021/acs.chemrev.9b00483

Zhao, X., & Deng, W. (2020). Printing photovoltaics by electrospray. Opto-Electronic Advances. https://doi.org/10.29026/oea.2020.190038

Zhou, M., Han, D., Cui, X., Wang, J., Chen, X., Wang, J., Sun, S., & Yan, W. (2024). Recent progress on advanced flexible lithium battery materials and fabrication process. Nanomaterials, 14(21), 1856. https://doi.org/10.3390/nano14221856